

Copyright Warning & Restrictions

The copyright law of the United States (Title 17, United States Code) governs the making of photocopies or other reproductions of copyrighted material.

Under certain conditions specified in the law, libraries and archives are authorized to furnish a photocopy or other reproduction. One of these specified conditions is that the photocopy or reproduction is not to be “used for any purpose other than private study, scholarship, or research.” If a user makes a request for, or later uses, a photocopy or reproduction for purposes in excess of “fair use” that user may be liable for copyright infringement,

This institution reserves the right to refuse to accept a copying order if, in its judgment, fulfillment of the order would involve violation of copyright law.

Please Note: The author retains the copyright while the New Jersey Institute of Technology reserves the right to distribute this thesis or dissertation

Printing note: If you do not wish to print this page, then select “Pages from: first page # to: last page #” on the print dialog screen

The Van Houten library has removed some of the personal information and all signatures from the approval page and biographical sketches of theses and dissertations in order to protect the identity of NJIT graduates and faculty.

ABSTRACT

In this research, an effort was made to better understand light-dark cycles which influence the physiological and psychological rhythms, circadian rhythms and their behavior. The research concentrated on mathematically modeling circadian rhythms (specifically hamsters' circadian activity rhythms) and establishing a physical correlation and creating a meaningful relationship between the mathematical model's parameters and the real biological oscillators which are responsible for these rhythms. The internal nature of the circadian rhythms is unclear. There is insufficient information and empirical data that describe them. Indirect means have to be employed for the description and exploration of such rhythms. Extensive real data analysis must be performed in the time and frequency domains and every possible aspect of the circadian rhythms should be investigated.

In our research, we studied and analyzed two types of circadian data, temperature and activity, which were extracted from rhesus monkeys and hamsters respectively by means of two separate data acquisition systems. The analysis which was accomplished in both the time and frequency domains revealed many important aspects of the circadian system and its characteristics. It was found that the circadian rhythms' period is approximately 24 hours. This period showed a small deviation when the animal was subjected to different environmental conditions (light, food, etc.). The frequency spectrum of the real circadian data showed its harmonics structure and revealed the existence of two distinct frequency components (bimodality).

Based on our analysis results and the knowledge of previous researchers work, we

developed a nonlinear two coupled-oscillator mathematical model to approach the real circadian data. The numerical solutions of the model were obtained by computer simulation and were compared to the real circadian data in both the time and frequency domains. Certain modifications of the model were necessary to achieve the desired outcome. These modifications not only included the changes in the value of the model's parameters, but also the addition of a high frequency oscillator. Later in the research, a periodic external stimulus was applied to the model in order to simulate entrainment. Our research has proven the ability of our mathematical model to simulate the circadian system.

**SIMULATION OF ACTIVITY RHYTHMS
IN THE HAMSTER**

**by
Paul Qassis**

Robert W. Van Houten Library
New Jersey Institute of Technology

**A Thesis
Submitted to the Faculty of
New Jersey Institute of Technology
in Partial Fulfillment of the Requirements for the Degree of
Masters of Science in Electrical Engineering**

Department of Electrical and Computer Engineering

January 1995

APPROVAL PAGE

SIMULATION OF ACTIVITY RHYTHMS
IN THE HAMSTER

Paul Qassis

Dr. Stanley Reisman, Thesis Advisor
Professor of Electrical Engineering, NJIT

_____ Date

Dr. John Ottenweller
Associate Professor of Neurosciences, New Jersey Medical School

_____ Date

Dr. Peter Engler
Associate Professor of Electrical Engineering, NJIT

_____ Date

BIOGRAPHICAL SKETCH

Author: Paul S. Qassis

Degree: Master of Science in Electrical Engineering

Date: January 1995

Undergraduate and Graduate Education

- Master of Science in Electrical Engineering.
New Jersey Institute of Technology,
Newark, New Jersey, January, 1995.
- Bachelor of Science in Electrical Engineering.
New Jersey Institute of Technology,
Newark, New Jersey, May, 1992.

Major: Electrical Engineering

This thesis is dedicated
to my parents, and Carissa

ACKNOWLEDGEMENT

I would like to express my appreciation and gratitude to Dr. Stanley Reisman for his assistance and support, without whose encouragement this work might never have been done.

TABLE OF CONTENTS

Chapter	Page
1 AN OVERVIEW	1
1.1 Introduction	1
1.2 Suprachiasmatic Nucleus	2
1.3 Circadian Rhythms (24 hour oscillations)	3
1.4 Mathematically Modeling Circadian Oscillators	4
1.5 Entrainment	5
2 TEMPERATURE AND ACTIVITY DATA	8
2.1 Circadian Data Acquisition	8
2.2 Data Acquisition System Overview	9
2.2.1 DATAQUEST III Overview	9
2.2.2 Infrared Module Overview	11
2.3 Pre-processing	14
3 DATA ANALYSIS	17
3.1 Frequency Analysis Tools	17
3.1.1 Zero Padding	17
3.1.2 Detrending	18
3.1.3 Windowing	19
3.2 Temperature data	20

TABLE OF CONTENTS
(Continued)

Chapter	Page
3.3 Activity Data (Light/Dark)	22
3.4 Activity Data (Dark/Dark)	25
3.5 Activity Data (Light/Light)	27
4 SIMULATION	29
4.1 Introduction	29
4.2 VISSIM	30
4.2.1 Van der Pol Oscillator and the Effect of μ (the nonlinear coefficient)	31
4.3 VisSim Mathematical Model	36
4.3.1 Coupled Van der Pol Oscillator	37
4.4 Velocity Coupling Simulation	41
4.5 Ultradian Rhythms	46
5 ENTRAINMENT	51
5.1 Introduction	51
5.2 Understanding Entrainment	53
5.3 Light/Dark to Dark/Dark Transition	59
5.4 Entrainment Simulation	62
5.5 Light/Light to Dark/Dark Transition	67

TABLE OF CONTENTS
(Continued)

Chapter	Page
6 CONCLUSION	69
6.1 Summary	69
6.2 What May Come ?	71
APPENDIX A	72
REFERENCES	81

LIST OF TABLES

Table	Page
4.1 The period of the Van der Pol oscillator with different values of μ	35
4.2 The correcting factors (ϵ_x, ϵ_y) needed for different (μ_x, μ_y) values	42

LIST OF FIGURES

Figure	Page
2.1 Data collection process overview.	10
2.2 Infrared Circuit Module.	11
2.3 Hamster's activity data. Each cycle is approximately 24 hours.	12
2.4 Monkey's temperature data. Each cycle is approximately 23.76 hours.	13
2.5 Temperature data of a Rhesus monkey prior to filtering.	15
2.6 The same temperature data as it appears after processing.	16
3.1 A 2000 point Hanning window.	19
3.2 Temperature record of a rhesus monkey.	20
3.3 Frequency Spectrum of the temperature data.	21
3.4 Records of 4 Hamsters' activity data placed in a light/dark environment (12h. light -12h. dark)	23
3.5 Frequency spectrum.	24
3.6 Activity data for 4 hamsters (Dark/Dark) environment.	26
3.7 Spectral functions of hamsters 17b, 18b, 27b, and 29b. The amplitude and structure of the fundamental periods and harmonics for the 4 hamsters are slightly different.	27
3.8 Activity data (Light/Light) for two different hamsters.. . . .	28
3.9 Frequency spectrum (Light/Light).	28
4.1 Time series waveforms of Van der Pol Oscillator: a) $\mu = 0$. b) $\mu = 0.2$. c) $\mu = .5$ d) $\mu=1$	32

LIST OF FIGURES
(Continued)

Figure	Page
4.2 Time series waveforms of Van der Pol Oscillator e) $\mu = 2$. f) $\mu = 5$	33
4.3 Spectral functions of the time series data obtained from VisSim. (a) $\mu=0$ (b) $\mu=0.2$ (c) $\mu=0.5$ (d) $\mu=1$ (e) $\mu=2$ (f) $\mu=5$. As μ is increased the period τ is increased.	34
4.4 Period deviation as μ increases.	35
4.5 Comparison of Frequency Spectrums. a) Real Activity data b) Spectral function . c) Single Van der Pol Oscillator Model with $\mu = 0.5$ (time series data) d) Spectral function.	38
4.6 a) Velocity coupling (time series). b) spectral function. c) direct coupling (time series). d) spectral function. In both coupling modes $F_{xy} = F_{yx} = 0.2$, and $\mu_x = \mu_y = 2$	40
4.7 Structural diagram and equations for a mathematical model of hamsters' circadian activity system.. . . .	43
4.8 A comparison between the simulation and the real circadian activity data in time and frequency domains.	42
4.9 A comparison between the simulation and the real circadian activity rhythm. The model's parameters were set to the following values: $F_{xy} = 0.5$, $F_{yx} = 0.2$, $\mu_x = 3.0$, and $\mu_y = 2.0$	45
4.10 A 100 point Sawtooth waveform.	47
4.11 Ultradian Rhythms simulation. The fundamental period is 8 hours.	48
4.12 a) hamster's activity data (Light/Dark) cycle. b) Simulation results after the addition of the ultradian oscillator.	49
4.13 a) Frequency spectrum of hamster's activity data (Light/Dark) cycle. b) Frequency spectrum of coupled Van der Pol oscillator model.	50

LIST OF FIGURES
(Continued)

Figure	Page
5.1 Activity data of various hamsters placed in different environments. a) Dark/Dark. b) Light/Dark. c) Light/Light	53
5.2 Spectral functions.	54
5.3 Time series simulation of the single Van der Pol oscillator model.	57
5.4 Time series simulation of the single Van der Pol oscillator with an external stimulus acting on it.	57
5.5 Spectral functions. a) Single Van der Pol oscillator, $\omega = 0.2856$ rad (22 hours) the natural frequency of the model. b) Single Van der Pol oscillator with an external stimulus applied to it. $\varpi = 0.2618$ rad (24 hours) the frequency of the external stimulus.	58
5.6 Time series activity data of an experimental hamster. The point labeled 2016 Sample is the point of transition from Light/Dark to Dark/Dark.	60
5.7 Time series plot of the activity data (light/dark to dark/dark transition). a) Light/dark b) Dark/dark.	60
5.8 Spectra light/dark to dark/dark transition. a) Spectra of the light/dark section which shows a fundamental period of 23.76 hours. b) Spectra of the dark/dark section which shows a fundamental period of 24.75 hours.	61
5.9 VisSim presentation of the Van der Pol coupled-oscillator model. The model include an external input which was applied and removed at specified intervals.	63

LIST OF FIGURES
(Continued)

Figure	Page
5.10 Structural diagram and equations for the final mathematical model..	64
5.11 Coupled oscillator model a) External input with a period of 24 hours was applied for 10 simulated days. The figure shows the fundamental frequency and the harmonics. b) After 10 simulated days the input was removed and the system was allowed to free-run.	65
5.12 Records of real circadian activity data..	66
5.13 Simulation output..	67
5.14 Frequency Spectrum of time series activity data. a) Light/Light before transition. b) Dark/Dark after transition.	68
5.15 Frequency spectrum of time series activity data during the transitional phase from Light/Light to Dark/Dark.	68

CHAPTER 1

AN OVERVIEW

1.1 Introduction

The theory of biorhythm states that from birth to death each of us is influenced by three internal cycles - the physical, the emotional, and the intellectual.^[10] Each cycle starts from a zero point and begins to rise in a positive phase, during which our energy and ability levels are both high. Gradually after reaching a peak point the cycle starts to decline towards the negative phase. During that phase, our energy level is replenished again. When the cycle reaches its negative peak, it begins to rise again toward the positive phase and the whole process repeats itself. Each cycle crosses the zero point midway through their complete periods. Our performance, physical or mental is a composite of these rhythms.

Circadian rhythms or biological clocks are the body's daily rhythms.^[8] The rhythms are self-sustaining biological oscillations which repeat themselves every day throughout our life. Such oscillations comprise the temperature and activity in humans and animals (observation that the temperature of the human body is not constant throughout the day was reported as early as 1736).^[4] Our bodies and minds are accustomed to these rhythms which in turn are affected by specific environmental cycles such as the light-dark cycles.

It is no secret that periodic phenomena exist and contribute to the coordination of

life-processes.^[6] The behavior of such systems in which every state is destined to recur at regular intervals has for so long been the interest of engineers, scientists and mathematicians. Many questions are encountered during the experimental study of biological rhythms such as: What is responsible for biological rhythms and their mechanisms? How can we recognize them if they were confronted? What are their physiological implications? and how can we mathematically model such systems?.

1.2 Suprachiasmatic Nucleus

Recently, a hypothesis has been accepted, which states that there are biological oscillators that exist in the living organisms and are responsible for the origination of biological rhythms.^[1] This was confirmed by an experiment which altered the basic biological rhythms of animals by transplanting brain tissue between hamsters with fundamentally different biological rhythms, which affirmed that a small area of the brain called the *suprachiasmatic nucleus* serves as the master clock. Normally, experimental hamsters wake up and start running approximately every 24 hours. When the suprachiasmatic nucleus was removed from the hamsters, the hamsters ran randomly at any time of the day or night. When the nucleus was implanted again, rhythms were restored. This experiment gave the idea of an existing organ controlling circadian rhythm.

Biological rhythms are not confined to a specific period or frequency. Biological rhythms with high frequency are called *ultradian*. These rhythms have short period oscillations (less than 16 hours) and such oscillations are apparent in various physical

waveforms such as the ECG (Electrocardiogram) which has an oscillation period between 0.1 - 5 seconds. Rhythms with a lower frequency are called *infradian* which have periods longer than 32 hours.

1.3 Circadian Rhythms (24 hour oscillations)

The term circadian comes from the Latin *circa*, meaning "about," and *die*, meaning "day" (About one day).^[8] Rhythms, or cycles, can be defined as repetitions at regular time intervals of situations, events, and levels of activity. A process that consistently repeats itself every 24 hours is one that has a daily rhythm. If this rhythm persists with approximately the same period in the absence or existence of any external time stimulus (*Zeitgeber*), it is called circadian rhythm. Circadian rhythms are self-sustaining (persist without a sign of damping) biological oscillations with a period of approximately 24 hours, they have been observed in the integrated organism and in cultured organs and tissues. Circadian rhythms are the rhythms of man's internal physiological clock or body clock. Perhaps, the most familiar biological rhythm is the light and dark rhythm of a period of 24 hours which controls the phases of sleep, or rest, and wakefulness. The circadian clock also measures the rhythm of when we are most sensitive to pain, and how well we estimate the passage of time.

Many experiments have been performed which substantiated the circadian oscillations existence. For example, experimental hamsters have been kept in a free-running and entrained environment (a free-running state exists when an external time

stimulus (zeitgeber) does not exist, while an entrained state exists when the external time stimulus is present and controls the period and phase of the rhythm). In the free-running case, all elements that might advise the hamsters about the time or light and darkness were abolished. The hamsters were kept in continuous dark or light. The hamsters exhibited periodicity which ranged from 23 to 25 hours in their behavioral activity. Similar experiments produced parallel results and confirmed the sustained and endogenous (internal oscillator within the organism) behavior of the circadian oscillators.

1.4 Mathematically Modeling Circadian Oscillators

Most models of circadian oscillators have been vague in defining their parameters in terms of physiological or biochemical processes since these rhythms' internal nature is still unclear. The Van der Pol oscillator is an example of one of these models since its terms and variables fail to identify or correlate to physiological occurrences but it exhibits certain dynamics similar to the internal mechanism of circadian rhythms.

All recent literature on circadian rhythms support the fact that the circadian processes are generated by more than one oscillator. Two separate oscillators were originally proposed by Pittendrigh to account for transient resetting patterns in the rhythm of pupal eclosion in fruit-flies.^[3] Pittendrigh proposed a model with two separate oscillators coupled to each other in a stable phase relationship that depends on the spontaneous frequencies of the two oscillators. This model was also proposed for the circadian activity rhythms in rodents. The model's purpose was to clarify the splitting of

the free-running rodents' activity rhythm into two distinct components which implied the existence of more than one oscillator.

Throughout this research we concentrated on a two coupled oscillator model.

$$K_y^2 \frac{d^2 y}{dt^2} + \mu_y K_y (Y^2 - 1) \frac{dy}{dt} + \omega_y^2 Y + F_{xy} \frac{dX}{dt} = 0 \quad (1.1)$$

$$K_x^2 \frac{d^2 x}{dt^2} + \mu_x K_x (X^2 - 1) \frac{dx}{dt} + \omega_x^2 X + F_{yx} \frac{dY}{dt} = 0 \quad (1.2)$$

Equations 1.1 and 1.2 are the mathematical representation of our basic model. In chapter 4, we will present the analysis and development of our model, and provide a comparison between the real time data and our computer simulation in both time and frequency domains. This does not imply that the circadian processes are generated by only two oscillators. We simply state an assumption. The circadian oscillators are complex in nature. At the present time there is insufficient empirical data from well-controlled studies to enable us to fully understand and provide complete analysis of these oscillators that are responsible for generating the biological rhythms. Although this is true, our model's results were promising. It exhibited many similarities to the hamster's real activity data in the time and frequency domain, which substantiated its potential for further future development.

1.5 Entrainment

As mentioned earlier, an entrained state exists when an external stimulus (Zeitgeber) is

present and controls the phase and rhythm of the endogenous biological oscillators. Biological oscillators, as many other non-linear oscillators, can be entrained. Circadian rhythms can only be entrained by periodic environmental time cues that are within 1-2 h of the free running period^[10]. For example, if we consider an endogenous free-running oscillator with a period of 23 hours, and we apply an external stimulus with a period of 24 hours to the free-running oscillator, the oscillator's period will shift towards the external stimulus period and synchronization will occur. This so called entrainment, will occur only if the external stimulus period is close to the free-running oscillator period or an integer multiple or submultiple of it. So, theoretically it is possible to change the rhythm of an oscillator and its period by applying to it the right stimulus with the proper amplitude, duration, and frequency. One of the applications to which entrainment can be applied is jet lag or jet syndrome. Jet syndrome is the result of circadian rhythm alteration which can be caused by shift work, transmeridian flight, or altered day length. It is an uncomfortable feeling which affects performance and well-being, including digestive disturbances and general malaise that could last for a few hours or a few days. The desynchronized individual may experience states of irritability, disorientation or confusion, distortion of time and distance, aches of various types, digestive upsets which include constipation, decrements of physical and mental efficiency, and disturbances in sleep habits. Considerable attention is focused on jet lag since it affects the ability to operate jet aircraft and manned spaced vehicles. There also has been a great deal of interest in trying to design schedules that would minimize the adverse effects of shift work on human health

and performance. ^[10] Circadian rhythms are believed to be disrupted when shift workers rotate from day to evening shift schedules or vice versa, which can cause internal temporal dissociation. Designing work schedules that would minimize the jet syndrome effect has been, and will be, a special concern. The disruption in the circadian rhythms is not only limited to internal desynchronization. It is believed that desynchronization from the external environment will also occur after a shift rotation because the worker might be asked to perform mental or physical activities at different times than is optimal according to his/her internal circadian clock. Many suggestions have been proposed in minimizing the jet syndrome effect on shift workers and the accelerated readjustment of the circadian clock. For example, Czeisler et al ^[12] has proposed a shift work schedule incorporating circadian principles. He suggested that work schedules should be rotated by lengthening the day (successive phase delays) instead of shortening it (successive phase advances). He supported the hypothesis with experiments which were performed on several shift workers, and demonstrated improvement in the adaptation rate of the workers to the new schedule.

It is extremely beneficial economically and medically to design a process that will minimize the side effects of such desynchronization and improve productivity. In principle, it is possible to design a special device with the right stimulus at the proper period, amplitude, and duration, that can be applied at the right time to disrupt the rhythm of the biological oscillator and change its period to synchronize to the new schedule, or the new time zone in the case of jet lag.

CHAPTER 2

CIRCADIAN TEMPERATURE AND ACTIVITY DATA

2.1 Circadian Data Acquisition

In order for any data acquisition system to be efficient, it should accumulate adequate and accurate information. To do so, enough information has to be gathered that can precisely describe the process at any instant. Needless to say, our collected data has to accommodate both.

Two types of circadian data, temperature and activity data, were acquired from rhesus monkeys and hamsters respectively by monitoring long term experiments. Long term experiments are needed because the period of the biological oscillators is approximately 24 hours (one cycle), so the length of the data recorded should be at least 240 hours (10 cycles) for each analysis. This long period of recording is essential for capturing adequate information needed from the temperature and activity rhythms for time and frequency analysis.

Accuracy on the other hand, is governed by many elements such as the sampling rate. The sampling rate should be high enough to be accurate, but at the same time it should not be too high to consume large storage capacity. We determined the sampling rate for our system to be 6 samples/hour. We believed that this sampling rate is practical and satisfies both requirements.

The activity experiments were performed primarily on hamsters. The hamsters

were kept in a controlled, isolated environment with food and water continuously available. It is very important for the experiment's environment to be well maintained in order to eliminate noise and other factors that might disturb the accuracy of the data. Also, all the factors that might inform the animals about time of day were eliminated. This is particularly important, since it inhibits any chance of the existence of external stimuli which might affect the free-running, self-sustained oscillators. As mentioned earlier, self-sustained oscillation means that oscillation will persist in the absence of any external stimulus and no damping will exist.

The temperature experimental data were acquired from Rhesus monkeys. These monkeys were kept in cages under carefully controlled light, temperature and noise conditions.^[1] The circadian rhythm of body temperature is a very important topic in physiological research since it involves both the regulation of body temperature and the mechanisms of biological timing. Also, since temperature is considered to be the most stable and regulated circadian rhythm, and since the phase of the temperature cycle is an important determinant of sleep onset and sleep length and has been linked to circadian performance effects, it becomes desirable to be investigated.

2.2 Data Acquisition System Overview

2.2.1 DATAQUEST III Overview

DATAQUEST III (Data Sciences Incorporation) is a hardware and software package that provides a tool for collecting and analyzing data from the laboratory. The system is

particularly effective in monitoring physiological data from laboratory animals. The strength of this system comes from its effectiveness in applications that require counting events, and its ability to log low frequency data signals such as temperature, heart rate, and oxygen consumption.

Since our application involves counting events (counting the revolutions of the running wheel as the hamster is running), the DATAQUEST III system was well suited. It provided us with continuous 24-hour monitoring of the hamsters' activity data and was capable for data online analysis. Also, the system provided 24 channels of data and enabled us to monitor many animals concurrently. Figure 2.1 is an overview of the system and its inter-connection.

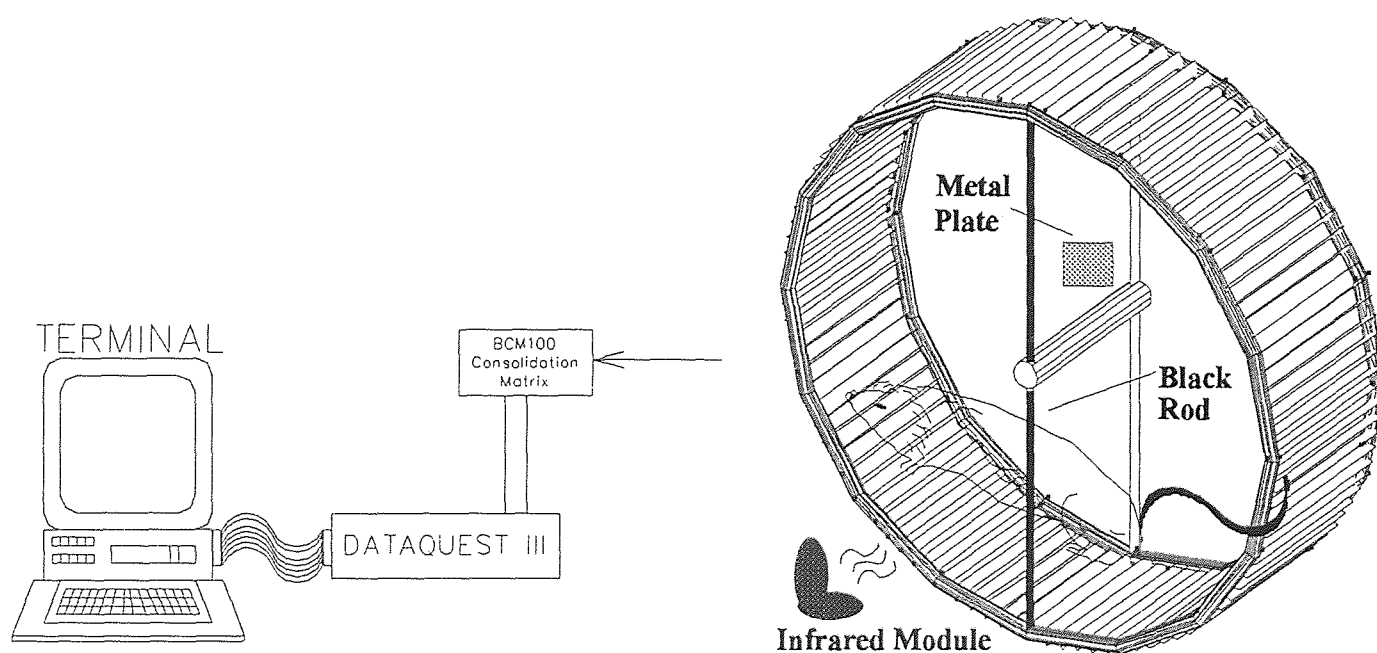


Figure 2.1 Data collection process overview.

2.2.2 Infrared Module Overview

The infrared LED transmits light onto the running wheel. Behind the running wheel there

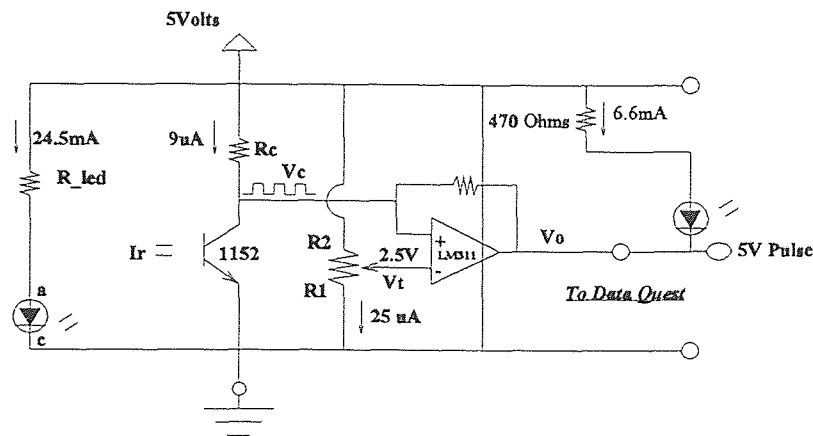


Figure 2.2 Infrared Circuit Module.

exists a metal piece that reflects the incident light, and on the front of the wheel is a vertical rod that has been painted in black in order to absorb the incident light and inhibit reflection. Depending on the actual position of the running wheel, light is reflected back to the infrared module or is absorbed through the black rod and reflection is inhibited. When the hamster is active and running, the running wheel is turning. Because of the nature of the system's structure, light is allowed to be reflected every half revolution interval. Hence, one point is collected every 1/2 revolution. When the light is reflected back to the infrared module, it energizes the infrared transistor (figure 2.2). The infrared transistor becomes active which results in V_c being low (≈ 0 V). As light is absorbed and

is not reflected back to the module, the transistor becomes inactive and this results in V_c being high ($\approx 1-3V$) by the action of the pullup resistor R_c and the cycle repeats itself. This alteration in the amplitude of V_c generates a pulse train. V_c is supplied to the positive input of the comparator and is compared to the comparator's threshold or reference voltage. The value of the threshold voltage V_t can be increased or decreased via a potentiometer. Typically, V_t is set to $2.5V$. As V_c exceeds the threshold voltage (V_t) the comparator's output V_o is high ($\approx 5V$). V_o is supplied to both, the LED and the DATAQUEST III system.

As mentioned earlier, each 1/2 revolution of the running wheel is represented by a pulse. DATAQUEST III accumulates the total number of pulses that have occurred during our sampling interval (6 samples/hours). When the sampling interval elapses,

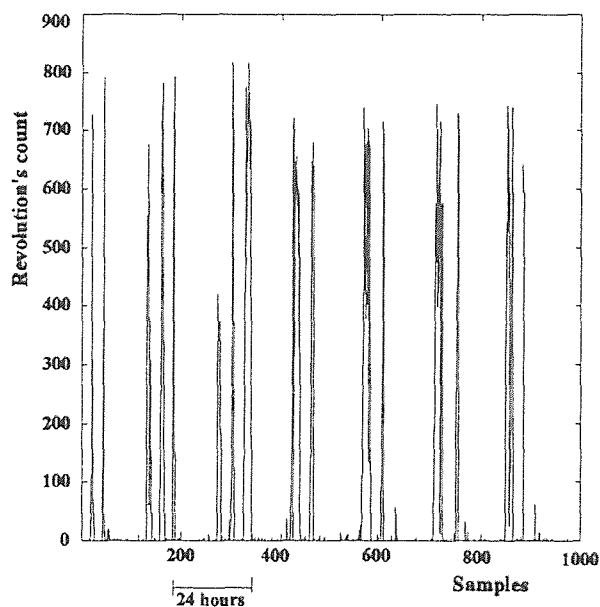


Figure 2.3 Hamster's activity data. Each cycle is approximately 24 hours.

DATAQUEST III stores the total count in a permanent record. In our case, the records were stored on the computer's hard disk. Figure 2.3 is an example of activity data obtained from the system.

Unlike the activity data, the temperature data were acquired from Rhesus monkeys.^[1] A separate acquisition system was developed at the VA Medical Center, East Orange, New Jersey. Figure 2.4 illustrates an overview of the circadian temperature data acquisition system and a sample plot of the data acquired.

TRANSMITTER—RECEIVER—FILTER—PULSE CONVERTER

PDP-11

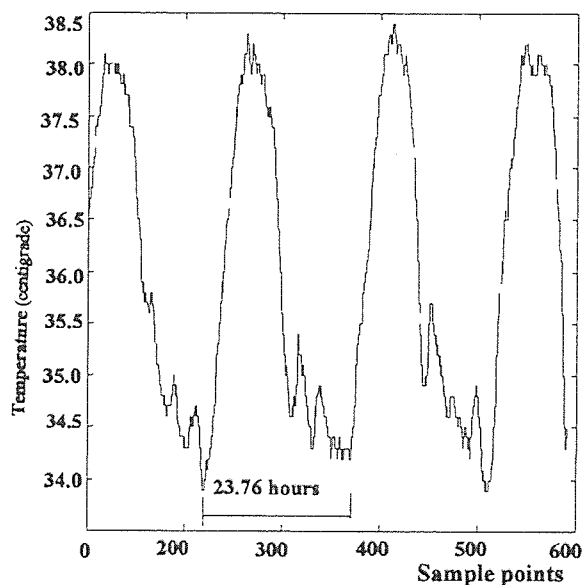


Figure 2.4 Monkey's temperature data. Each cycle is approximately 23.76 hours.

The monkeys were kept in cages in a well controlled environment (lights, temperature, and noise). Two types of experiments (free-running, or entrainment) were performed. This was accomplished by controlling the lights and their duration in the cages either by a timer or computer controlled switches. The monkey's temperature was transmitted from his body by means of a temperature transducer and transmitter module (carrier frequency 27 - 28 MHz) which were surgically implanted in the monkey's body. At room temperature, pulses were transmitted from the module at a rate of 100 - 200 pulses/min to the SONY ICE-2010 PLL synthesized high sensitivity receivers. The signal was then passed to an analog low-pass receiver (3dB cut off at 1 kHz for noise filtering) and subsequently transferred to the PDP-11 computer. The PDP-11 counted and stored the pulses received during a 2 minute segment in each 10 minute interval, producing a sampling rate of 144 samples/24hr.

2.3 Pre-processing

Since the two types of data (temperature and activity) differ in nature, different methods of data pre-processing were applied. Data pre-processing is required since the raw data may be accompanied by noise and some interruption even in a controlled environment. Such pre-processing may involve filtering, and averaging or other means. Although the two types of data differ they exhibit one similarity which is their periodicity. The period of these rhythms varied between 22 and 26 hours.

Filters are most often used to enhance signals by removing unwanted components

from them such as noise. Unlike the activity data, temperature data was subjected to interruption and contained noise interference. A specially designed filter was created to accomplish the task of noise removal. Since our temperature data points have a certain amplitude range, data points that were out of the normal range were eliminated. In order to accomplish this task, a five data points window was created. Data points' amplitude within the window were compared to each other and averaged, thus eliminating the very high or very low amplitude data points (can be related to noise interference). Then, the window would be moved by one data point increment and the process repeated until the end of the data file. This process is often referred to as scaling. The filter was written in C language and the program is listed in appendix A.

Figure 2.5 shows the temperature data of a rhesus monkey prior to any pre-processing and noise removal. Figure 2.6 shows the same temperature data after pre-processing.

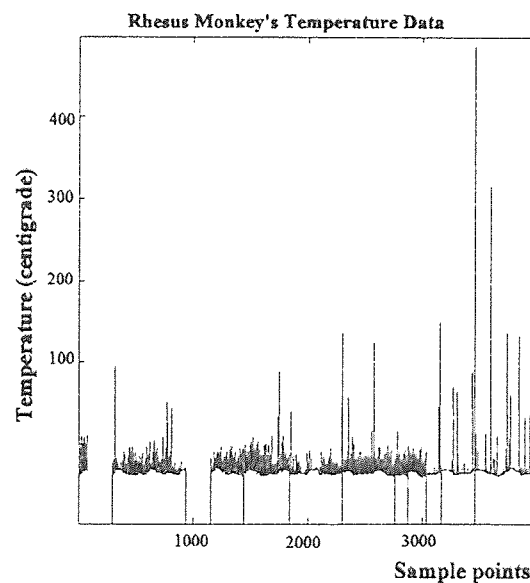


Figure 2.5 Temperature data of a Rhesus monkey prior to filtering.

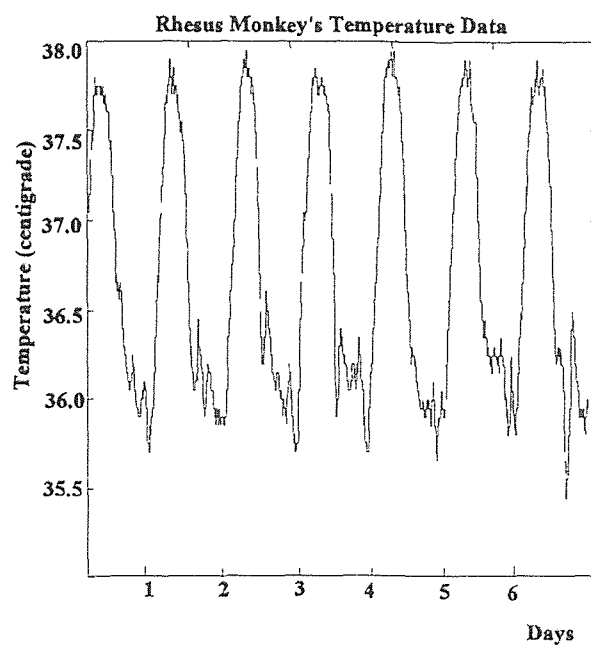


Figure 2.6 The same temperature data as it appears after processing.

CHAPTER 3

FREQUENCY ANALYSIS

3.1 Frequency Analysis Tools

Spectral analysis on the activity and temperature data was performed using the FFT. FFT (Fast Fourier Transform) is an algorithm for computing the discrete Fourier transform of a data series at all of the Fourier frequencies. Fourier analysis can be treated as a decomposition of the time series into a sum of sinusoidal components.

Prior to performing the FFT on the time series set of data, certain frequency analysis techniques have to be employed in order to significantly increase the accuracy of the outcome.

3.1.1 Zero Padding

Zero padding was incorporated to extend the data length. Zero padding is used to enhance the resolution of the frequency spectrum. The frequency resolution is

$$\Delta f = \frac{1}{T} \quad (3.1)$$

Where:

Δf = Frequency in Hz

T = Length of signal in seconds

As we increase the length of the signal by the addition of zero points at the beginning or the end of the data series, the precision of the frequency resolution will significantly improve.

As mentioned earlier, temperature and activity data were obtained at a sampling rate of 6 samples/hour. As a result, the sampling frequency is determined by the following:

$$\Delta F = 6 \frac{\text{samples}}{\text{hour}} \times \frac{1 \text{ hour}}{60 \text{ minutes}} \times \frac{1 \text{ minute}}{60 \text{ seconds}} = 0.00167 \text{ samples/sec.}$$
 If we use 1024 points for the Fourier transform, the frequency resolution is 8.134×10^{-7} samples/sec, but will be reduced to 5.09×10^{-9} samples/sec. if 16384 points are used. ^[1]

3.1.2 Detrending

Detrending, a process which involves the removal of the low frequency components was also applied to the circadian data. Since very low frequency components ($0 - 2.5 \times 10^{-6}$ Hz) may seriously affect the amplitude of the desired signal in the frequency domain, they either have to be removed, or the data frequency spectrum can be plotted following the low frequency components therefore ignoring their effect. Several factors can cause these low frequencies such as the instruments used, or the long term trend of data (monkey's circadian rhythms). The circadian activity data contained minimal low frequency components and noise. This was due to the nature of the acquisition system (counting the revolutions of the running wheel), unlike the temperature data acquisition system which was subjected to varying forms of interference. Therefore, the frequency spectrum of the circadian activity data was not smeared at low frequencies. In order to eliminate any

possibility of a low frequency component affecting our power spectrum, the power spectrum was usually plotted excluding the first 20 points. This method should be used with care in order not to bypass the real data's desired signal.

3.1.3 Windowing

In this research, a Hanning window was used in order to increase the smoothness of the Fourier transform and to limit the duration of the time series data. The Hanning window is defined as:

$$\omega(t) = \cos^2 \frac{\Pi t}{T} = 0.5 \left(1 + \cos \frac{2\Pi t}{T} \right), \text{ where } |t| \leq \frac{T}{2} \quad (3.2)$$

In the time domain, windowing is accomplished by multiplying $\omega(t)$ by our time series data.

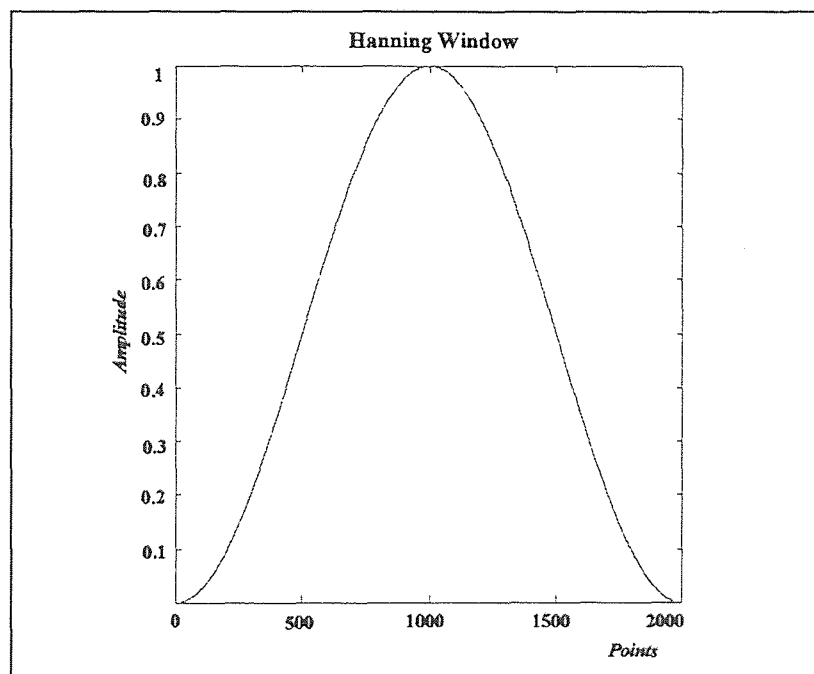


Figure 3.1 A 2000 point Hanning window.

Figure 3.1 shows an example of a Hanning window with an amplitude of 1 and a duration of 2000 points. Depending on the desired length of data transformed, the duration of the window can be increased or decreased.

3.2 Temperature data

Body temperature oscillates on a daily basis. A consistent elevation of body temperature during daytime, and lowering during nighttime occurs. For example, in human beings under natural conditions of lighting and social interaction, with wakeup time at 7 a.m. and bedtime at 11 p.m., body temperature starts rising from the nighttime low of approximately 36.5°C by 9 a.m. keeps rising slowly to a peak of 37.4°C at about 2 p.m. and then falls to reach the initial level of 36.5°C at 4 a.m. ^[4] We obtained temperature data from several rhesus monkeys. Figure 3.2 shows a plot of one of the temperature

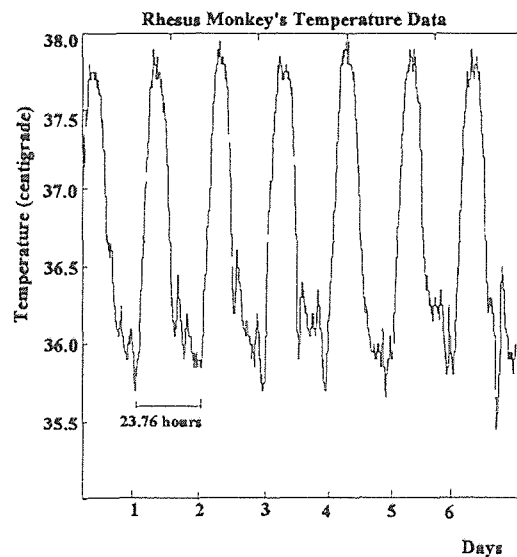


Figure 3.2 Temperature record of a rhesus monkey.

records acquired. The duration of each cycle was slightly under 24 hours (23.76hr.). The period stability of the core temperature rhythm was consistent. This stability enabled us to accurately determine the period of each rhythm.

To further explore the data, their spectral functions must be analyzed. The spectral function allows us to identify and measure frequencies (fundamental and harmonics) and their amplitude. Phases of decomposed sinusoids in a time series are more apparent in the frequency domain than the time domain. Consequently, spectral analysis provides a tool to better understand the characteristics of the system.

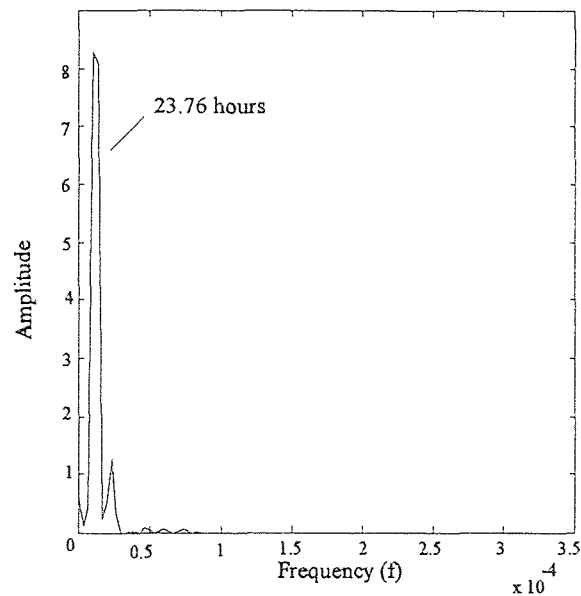


Figure 3.3 Frequency Spectrum of the temperature data.

Figure 3.3 shows the frequency spectrum of the temperature record of a rhesus monkey shown in figure 3.2 where the main frequency component (fundamental frequency) peak occurred at $\approx 1.17 \times 10^{-5}$ cycle/sec. The following computations will

determine the period of the cycle:

$$1.17 \times 10^{-5} \frac{\text{cycles}}{\text{second}} \times \frac{60 \text{ seconds}}{1 \text{ minute}} \times \frac{60 \text{ minutes}}{1 \text{ hour}} = 0.04212 \frac{\text{cycle}}{\text{hour}}$$

$$\frac{1}{0.04212 \frac{\text{cycle}}{\text{hour}}} = 23.76 \frac{\text{hours}}{\text{cycle}}$$

all future discussion will be focused on activity circadian rhythms. This evolved from the following reasons:

- Temperature circadian rhythms have been analyzed and simulated by previous researchers.^[1]
- Activity circadian data was available and was easy to obtain.
- Many interesting experiments have been performed to obtain various types of circadian activity data (free-running, and under different entrainment conditions).

3.3 Activity Data (Light/Dark)

Figure 3.4 shows plots of hamsters' activity data (time series). The four hamsters were exposed to a 12hr.-light/12hr.-dark environment (entrained condition). Further analysis of the experimental data emphasizing their frequency characteristics is depicted in figure 3.5.

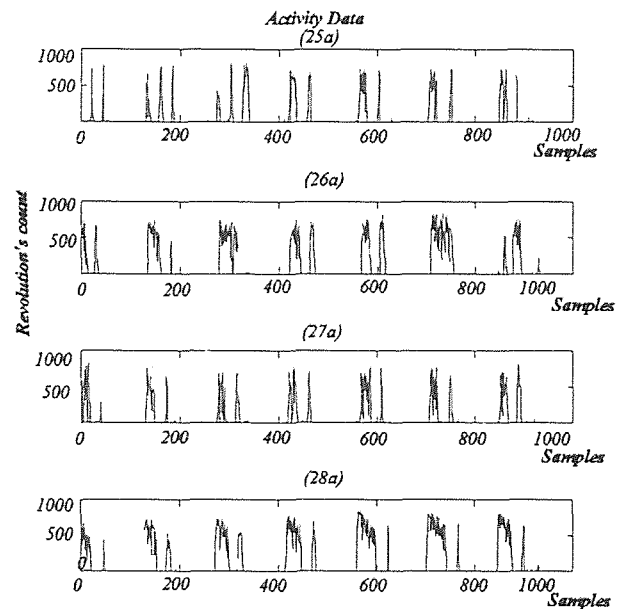


Figure 3.4 Records of 4 Hamsters' activity data placed in a light/dark environment (12h. light - 12h. dark)

The spectrum shows the fundamental frequencies and the 2nd, 3rd and higher harmonics. The fundamental period was derived from the fundamental frequency as follows:

Since the fundamental frequencies of the 4 hamsters were = 1.156×10^{-5} cycle/second,

$$1.156 \times 10^{-5} \times 3600 \frac{\text{seconds}}{1 \text{ hour}} = 4.16 \times 10^{-2} \text{ cycle/hour}, \quad \frac{1}{4.16 \times 10^{-2} \text{ cycles / hour}} = 24.02 \text{ hours/cycle.}$$

Our spectral analysis results show that the circadian rhythms structure of temperature and activity consist of harmonics and sub-harmonic frequencies. Although the amplitudes and shapes of the harmonics differed, their frequency peak occurred at 2.312×10^{-5} , 3.481×10^{-5} , and 4.623×10^{-5} cycles/sec. consecutively. Similar computations were performed in order to

determine the period of each harmonic. Results are shown in figure 3.5.

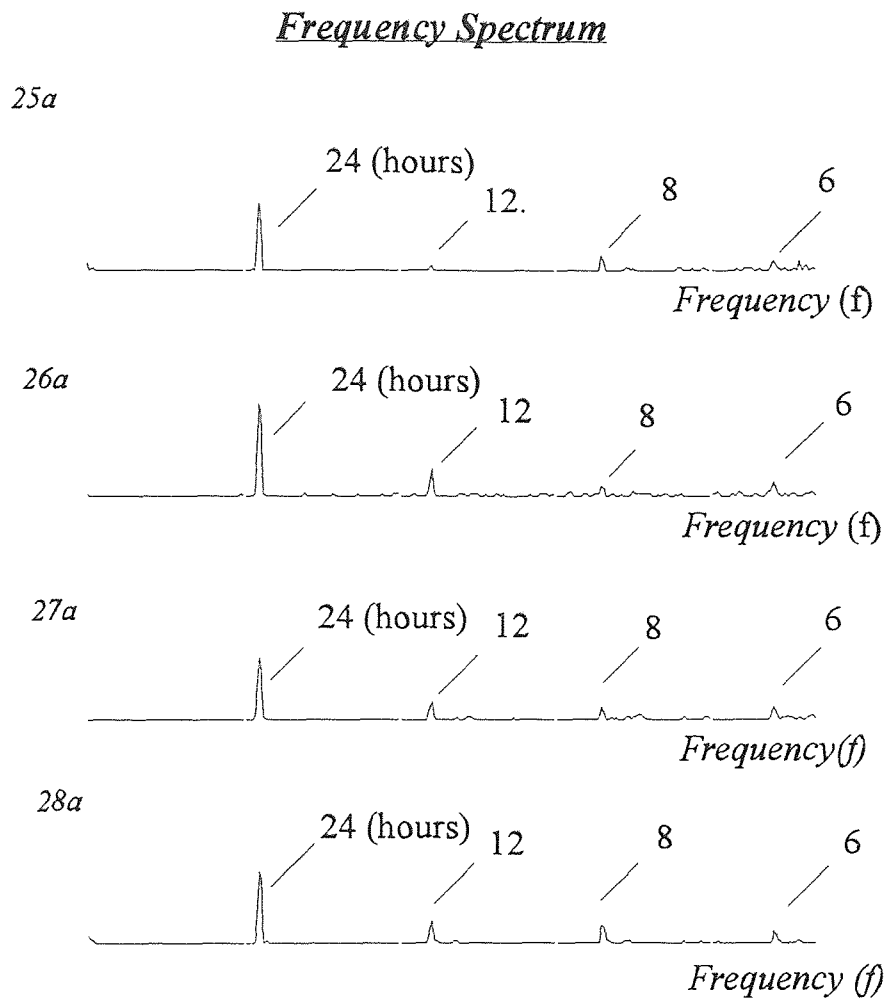


Figure 3.5 Frequency spectrum.

Many studies measured activity and body temperature simultaneously and their rhythms exhibit very similar characteristics. The high phase of the temperature circadian rhythms coincided with the active phase of the activity circadian rhythm.^[4] Since physical

activity can raise the body temperature, one might think that the temperature circadian rhythm is a consequence of the activity circadian rhythm. Although this discussion appears to be valid, facts on the other hand, suggest that the two rhythms are independent but maybe controlled by the same timing mechanism. First, body temperature in humans and animals starts to rise before the subject wakes up and becomes active. Second, studies in humans showed that it is possible to maintain the same level of activity during the full circadian cycle. Finally, it has been found in several studies that some subjects, under some conditions, may show a dissociation of the two rhythms so that the two rhythms proceed with different periods and , consequently, with a constantly changing phase relationship. These studies suggest that despite the fact that body activity and exercise can affect body temperature, body temperature circadian rhythm is not merely a result of circadian rhythm of activity and is generated independently.

3.4 Activity Data (Dark/Dark)

All lights were extinguished and the hamsters were placed in a completely dark environment. This experiment was performed in order to eliminate any simulated environmental synchronizing cycles (zeitgeber) and allow the hamsters to free-run. Figure 3.6 shows plots of the activity data obtained. Figure 3.7 shows the spectra transformed from these activity circadian rhythms under free-running circumstances.

Hamsters (17b & 18b) show a fundamental period of 24.3h., while hamsters (27b & 29b) show a fundamental period of 24.03h.

$$1.143 \times 10^{-5} \frac{\text{cycle}}{\text{second}} \times 3600 \frac{\text{seconds}}{\text{hour}} = 0.0411 \frac{\text{cycle}}{\text{hour}} = 24.3 \frac{\text{hours}}{\text{cycle}}$$

$$1.156 \times 10^{-5} \frac{\text{cycle}}{\text{second}} \times 3600 \frac{\text{seconds}}{\text{hour}} = 0.0416 \frac{\text{cycle}}{\text{hour}} = 24.03 \frac{\text{hours}}{\text{cycle}}$$

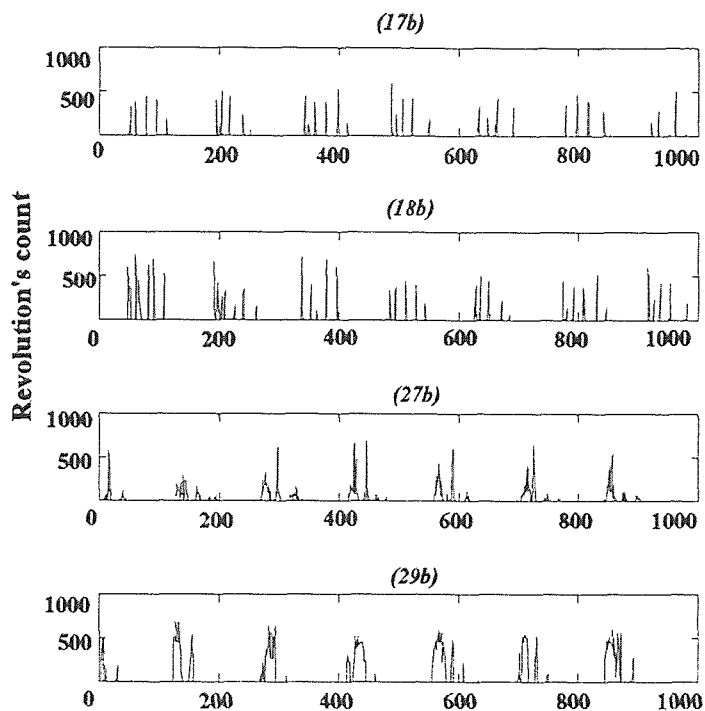


Figure 3.6 Activity data for 4 hamsters (Dark/Dark) environment.

Unlike the spectra of the light/dark environment, which showed a consistent fundamental period of 24 hours, the fundamental period for hamster 17b & 18b was slightly different from the fundamental period of hamsters 27b & 29b. This fact becomes particularly important when we discuss entrainment in detail in chapter 5.

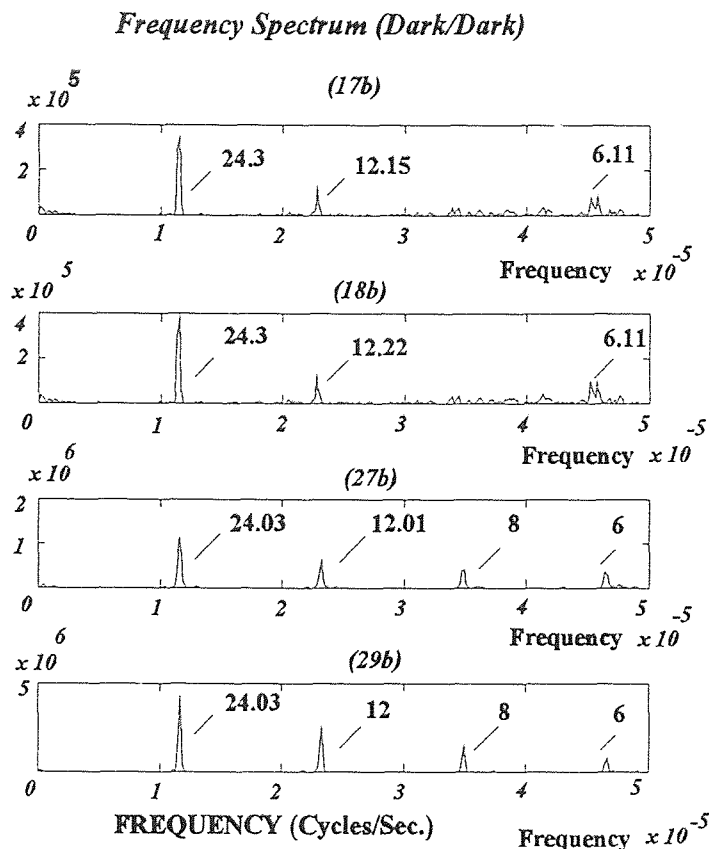


Figure 3.7 Spectral functions of hamsters 17b, 18b, 27b, and 29b. The amplitude and structure of the fundamental periods and harmonics for the 4 hamsters are slightly different. The 3rd harmonic for a and b is not obvious while it is evident in c and d.

3.5 Activity Data (Light/Light)

Figure 3.8 shows the activity rhythms for hamsters 31a, 33a who were in a free-running condition (light/light environment). Figure 3.9 shows the spectral functions of the two hamsters. The fundamental frequency for both hamsters is 1.13×10^{-5} cycles/sec., and the 3 harmonics occurred at 2.273×10^{-5} , 3.403×10^{-5} , and 4.532×10^{-5} cycles/sec. respectively. The fundamental period is 24.582 hours. Both spectral functions show clear 2nd, 3rd and 4th harmonics. Although the harmonic structure is similar, they had different amplitudes.

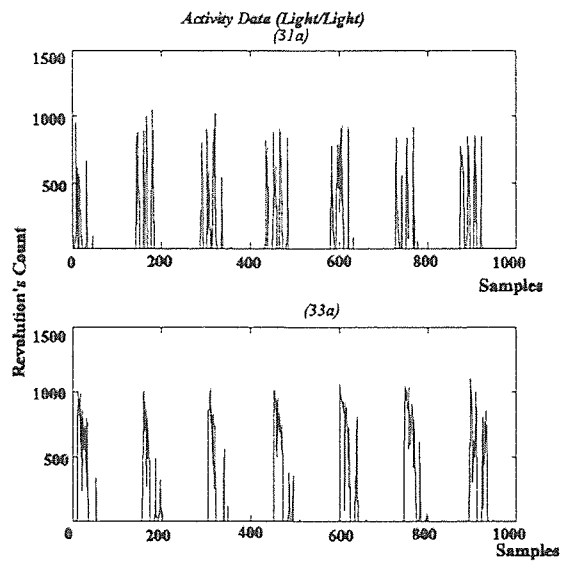


Figure 3.8 Activity data (Light/Light) for two different hamsters..

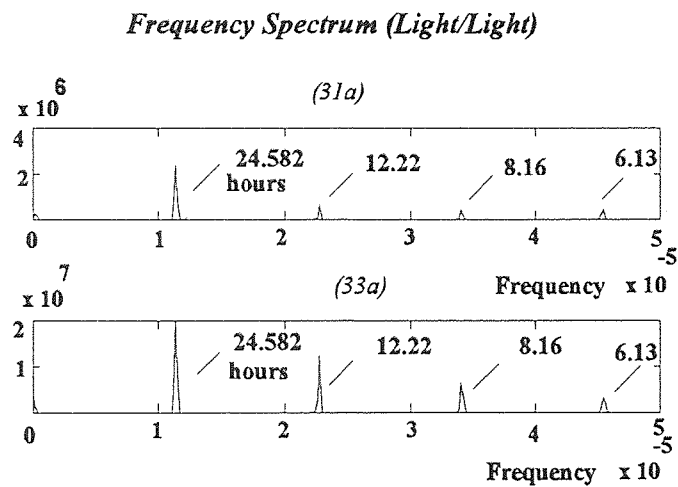


Figure 3.9 Frequency spectrum (Light/Light).

CHAPTER 4

MATHEMATICAL MODELING

4.1 Introduction

Modeling of systems serves as a useful tool to understand and describe especially unclear processes. It allows the development and the establishment of optimized mathematical equations. Optimization is accomplished by the iteration process (by adjusting the model and its parameters repeatedly). Modeling also provides us with the ability to perform certain tests which normally would present a risk to animals or humans.

In this research, we emphasize the modeling of circadian activity rhythms. The output of our simulated model should be equivalent, or closely related to, the real experimental activity data in both the time and frequency domains. In summary, our model should accomplish the following tasks:

- Simulate and describe the biological process that is responsible for the activity circadian rhythm and other biological rhythms.
- Provide us with the ability to investigate special properties and characteristics of the biological system.
- Possess flexibility to the addition of mathematical modules that describe complicated phenomena, such as entrainment and desynchronization.

Previous researchers pointed out that circadian rhythms may be generated by nonlinear oscillators, specifically, two coupled oscillators. For example, Phillipa Gander,

Richard Kronauer, Charles Czeisler and Martin Moore-Ede created a coupled Van der Pol oscillator model that describes the action of zeitgebers on the human circadian system.^[12]

Shi Xiong Yang developed a two coupled oscillator model to describe the temperature circadian system of rhesus monkeys.^[1] These researchers and others created mathematical models for the circadian rhythms which exhibit the following properties:

- The endogeneity in circadian rhythms (self-sustainment).
- More than one oscillator is responsible for circadian rhythms which are coupled to each other (direct coupling, velocity coupling, etc.).
- The coupled oscillators are of Van der Pol oscillator type.
- The oscillators are nonlinear with varying levels of nonlinearity.

We will include all of these common features in our model. In addition, we will include an external stimulus that will simulate the action of zeitgebers and investigate entrainment. Also, we will simulate ultradian rhythms accompanied by noise (higher frequency rhythms) that may be responsible for the intermittency of the activity cycles. Chapter 5 will discuss these features in detail.

4.2 VISSIM

VisSim is a modeling software that uses graphical interface and is available on the MS/Windows and UNIX/X computer platforms. VisSim, provides the ability to design, simulate and plot mathematical models. VisSim provides the user with its own function blocks such as integration, summation, limiters, etc,. Also, it enables the user to create and implement his/her own custom block functions using C, Pascal, or Fortran.

In this research, VisSim was used for the coupled oscillator model simulation. All the simulation time series data were acquired from the simulation model and were saved as ASCII files. The ASCII files were then exported to MatLab and all the frequency analysis was performed using MatLab. Refer to appendix A for an example of a single Van der Pol oscillator simulation.

4.2.1 Van der Pol Oscillator and the Effect of μ (The nonlinear coefficient)

In order to better understand the mathematical model and the effect of μ (the non-linearity parameter) on the period and the overall system, the one dimensional Van der Pol oscillator was first simulated and analyzed with different μ values.

$$K^2 \frac{d^2x}{dt^2} + \mu K(x^2 - 1) \frac{dx}{dt} + \omega^2 x = 0 \quad (4.1)$$

$\mu =$ *The non-linearity parameter*

$K =$ *Fixed time parameter*

$\omega =$ *Characteristic frequency of the system*

K is used to normalize the characteristic frequency of the system, such that for $\omega = 1$ the

$$\omega = \frac{2\pi}{T} \quad (4.2)$$

system has a period of 24 hours, and for $T = 24$ hours:

$$K = \frac{24}{2\pi} \quad (4.3)$$

As μ is increased the non-linearity of the system increases and as μ is decreased the non-linearity of the system decreases. If we let $\mu = 0$, the system becomes a linear system.

Figures 4.1 and 4.2 show plots of the waveforms that were obtained from the simulation using different μ values.

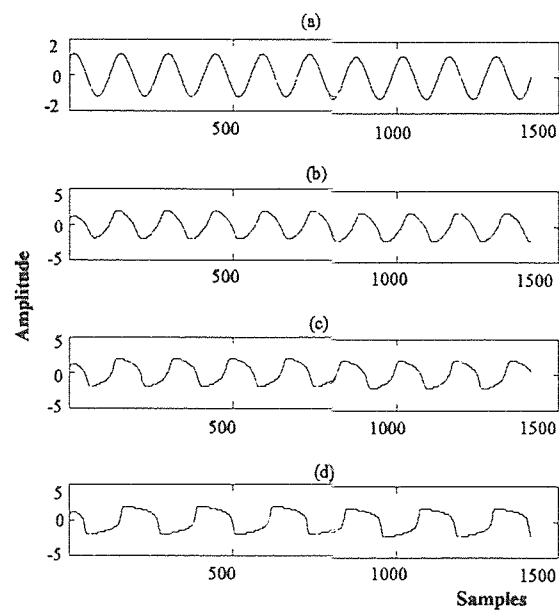


Figure 4.1 Time series waveforms of Van der Pol Oscillator: a) $\mu = 0$. b) $\mu = 0.2$. c) $\mu = .5$ d) $\mu = 1$

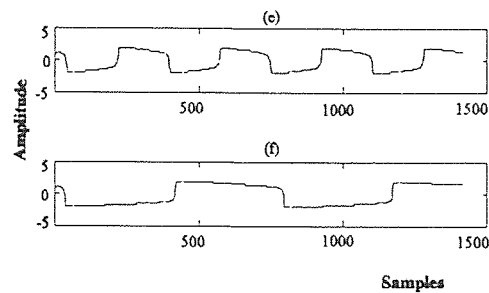


Figure 4.2 Time series waveforms of Van der Pol Oscillator e) $\mu = 2$. f) $\mu = 5$.

To acquire the numerical solution of the system, the Van der Pol oscillator was simulated using VisSim. The numerical solution (time series data) of the simulation was saved as an ASCII file and exported to MatLab. The FFT (Fast Fourier Transform) was then performed on the data to transform it to the frequency domain. Figure 4.3 shows the spectra of the time series data for different values of μ shown in figures 4.1 and 4.2.

As μ was increased from 0 to 5, the period increased from 24 hours to 126.23 hours. Also, higher order harmonics became more obvious as the nonlinearity coefficient was increased. The results can be summarized as follows:

- With $\mu = 0$, the output waveform of the Van der Pol oscillator was a cosine-like waveform with a period of 24 hours. As μ increased, the output waveform deviated from the cosine-like waveform.
- The period of the system increased as μ increased, and became large as μ became large.

- As μ increased from a zero value, the output waveform and harmonic structure of the Van der Pol oscillator began to resemble the real circadian data waveform and its harmonic structure.

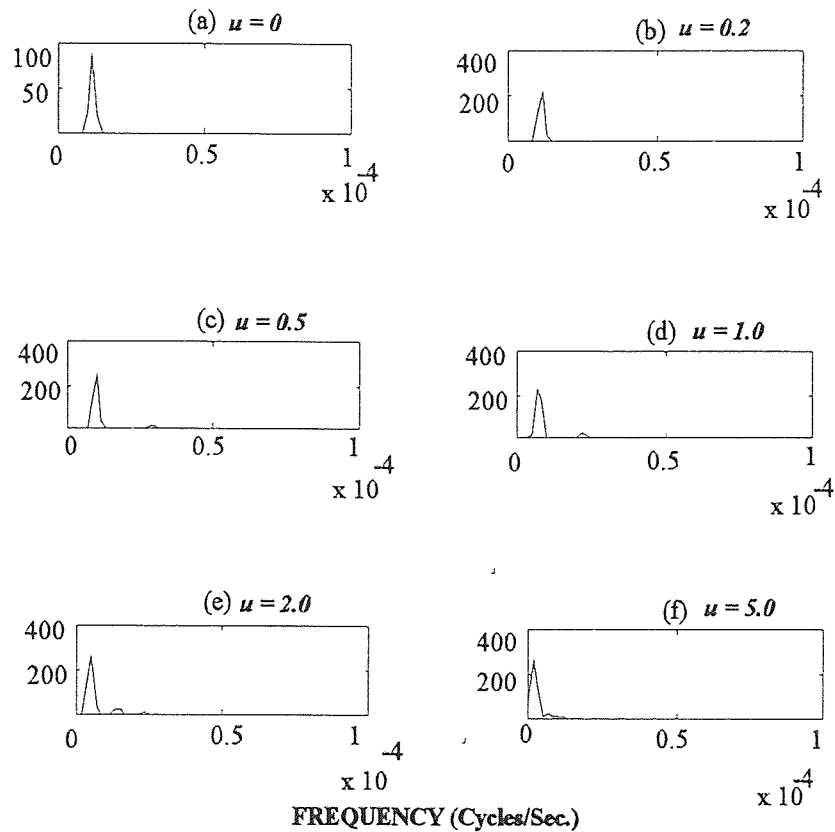


Figure 4.3 Spectral functions of the time series data obtained from VisSim. (a) $\mu=0$ (b) $\mu=0.2$ (c) $\mu=0.5$ (d) $\mu=1$ (e) $\mu=2$ (f) $\mu=5$. As μ is increased the period T is increased.

- The amplitude of the fundamental frequencies and the harmonic components increased as μ increased.

The following table compares the various values of the system's fundamental period as a result of different μ values.

μ	T
0	24
0.2	25.46
0.5	25.88
1	38.09
2	58.84
5	126.23

Table 4.1: The period of the Van der Pol oscillator with different μ values.

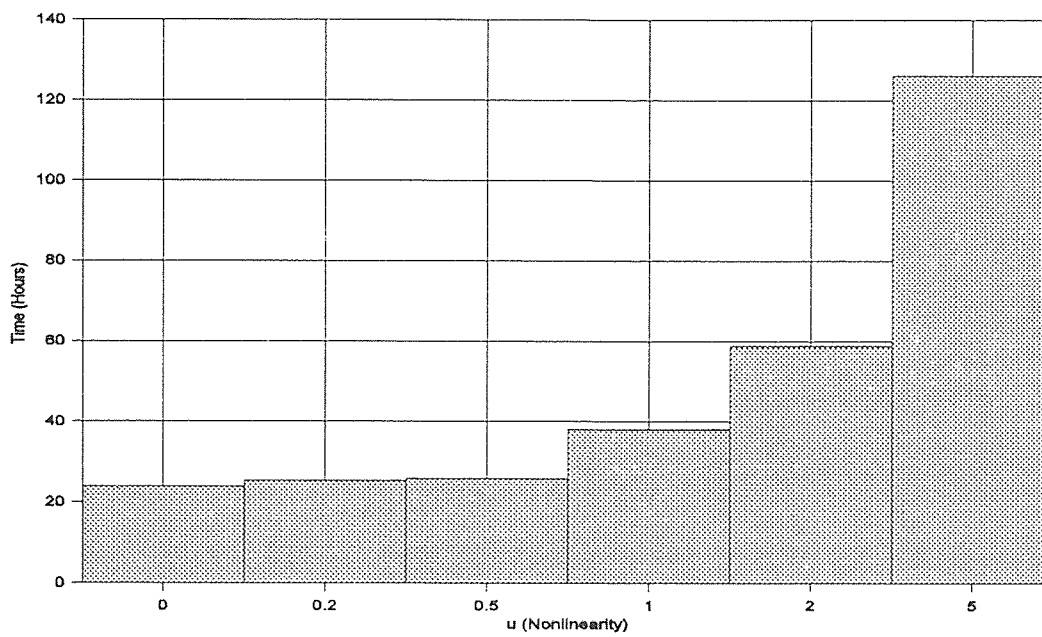


Figure 4.4 Period deviation as μ increases.

As mentioned earlier, the oscillator's fundamental period increased as μ increased.

In order to restore the original fundamental period of the oscillator, we multiplied the oscillator's frequency (ω^2) by a correcting factor (ϵ) which was determined empirically.

For example, when μ was set to 1.0, the period of the oscillator increased from its original value (24 hours) to 38.09 hours. We multiplied the term ω^2 by an ϵ value of 1.8 (increasing the frequency, decreases the period) which restored the fundamental period to its original value (24 hours). This is particularly essential for our coupled-oscillator model (section 4.3.2), since the coupling of the oscillators will also produce an effect on the period of the output, we needed to isolate the two effects (the effect of μ and the coupling).

4.3 VisSim Mathematical Model

The circadian system is assumed to be composed of a dual-oscillator mechanism which drives secondary oscillators responsible for the expressions of circadian rhythms. This suggests that any given circadian rhythm is jointly controlled by two endogenous oscillators. As mentioned in section 4.1, a coupled Van der Pol oscillator was used to generate an outcome similar to the circadian activity rhythm. Different means of coupling methods (direct or position coupling, velocity coupling)have been employed in an effort to determine the best model that will approximate the circadian system. Also, the model was expanded to include an external stimulus "Zeitgeber" which simulates the light stimulus applied to the subject and induces its external rhythm with a 24 hour cycle on the internal oscillator to entrain it. Other interesting prospects were introduced in the model which included the relaxation and ultradian oscillator theories.

4.3.2 Coupled Van der Pol Oscillator

$$K_y^2 \frac{d^2 y}{dt^2} + \mu_y K_y (Y^2 - 1) \frac{dy}{dt} + \omega_y^2 Y + F_{xy} \frac{dX}{dt} = 0 \quad (4.4)$$

$$K_x^2 \frac{d^2 x}{dt^2} + \mu_x K_x (X^2 - 1) \frac{dx}{dt} + \omega_x^2 X + F_{yx} \frac{dY}{dt} = 0 \quad (4.5)$$

where:

μ_x = nonlinear coefficient of the x oscillator.

μ_y = nonlinear coefficient of the y oscillator.

K = normalized time constant.

F_{xy}, F_{yx} = coupling coefficients.

By adding a second oscillator, coupling functions (F_{xy}, F_{yx}), different coupling modes (velocity or direct coupling), and additional nonlinear coefficients (μ_x) are introduced to the model. These additions might help us in producing the desirable time series and spectral structures. In order for our model to replicate as closely as possible the hamster's activity data, the oscillator (primary Y) had to be coupled to another oscillator (Secondary X). The most logical evidence for the use of a coupled oscillator model is the existence of two distinct frequency components. This occurrence of two sharply defined non-harmonic frequencies is not evident in a single oscillator. Figure 4.5 illustrates the difference between the time and frequency domains of the single Van der Pol oscillator model and the hamster's activity data.

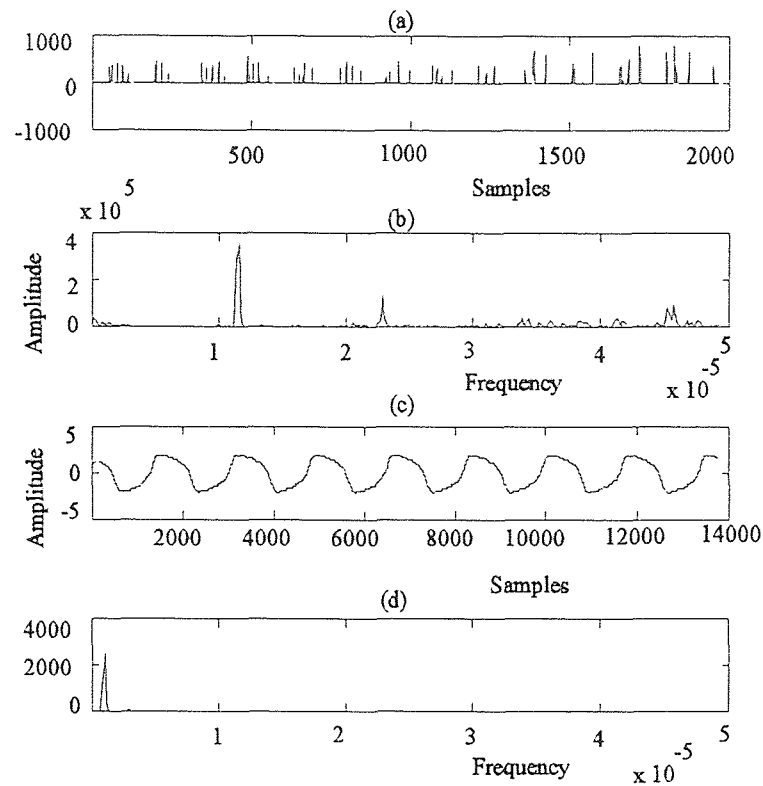


Figure 4.5 Comparison of frequency spectrums. a) Real activity data b) Spectral function . c) Single Van der Pol oscillator model with $\mu = 0.5$ (time series data) d) Spectral function of the Van der Pol oscillator model.

A model for circadian pacemakers consisting of two coupled oscillators has been proposed by Pittendrigh and Daan ^[6] in qualitative terms. The basic propositions of this model are the following:

Since it was not possible for a single oscillator to simultaneously produce two sharply defined non-harmonic frequencies, and because the free-running activity rhythms in rodents splits into two distinct components, two separate oscillators (X and Y) coupled to each other in a stable phase relationship (ϕ_{EM} , established prior to coupling) are

assumed to be responsible for the rhythms. The two oscillators control the onset and end of activity (evening and morning peaks respectively) in nocturnal animals. The period of the system (T) changes as the phase relationship is changed.

In our model, we investigated two types of coupling (velocity and direct coupling).

The following two equations are an example of a direct coupling model:

$$K_y^2 \frac{d^2 y}{dt^2} + \mu_y K_y (Y^2 - 1) \frac{dy}{dt} + \omega_y^2 Y + F_{yx} X = 0 \quad (4.6)$$

$$K_x^2 \frac{d^2 x}{dt^2} + \mu_x K_x (X^2 - 1) \frac{dx}{dt} + \omega_x^2 X + F_{xy} Y = 0 \quad (4.7)$$

The following two equations are an example of a velocity coupling model:

$$K_y^2 \frac{d^2 y}{dt^2} + \mu_y K_y (Y^2 - 1) \frac{dy}{dt} + \omega_y^2 Y + F_{yx} \frac{dX}{dt} = 0 \quad (4.8)$$

$$K_x^2 \frac{d^2 x}{dt^2} + \mu_x K_x (X^2 - 1) \frac{dx}{dt} + \omega_x^2 X + F_{xy} \frac{dY}{dt} = 0 \quad (4.9)$$

The two modes of coupling have similar effects on the system, but velocity coupling is much weaker than the direct coupling mode. For example, in the direct coupling system, the primary oscillator Y showed a stronger influence on the frequency of the secondary oscillator x, and sub-harmonic entrainment was more apparent (figure 4.6).

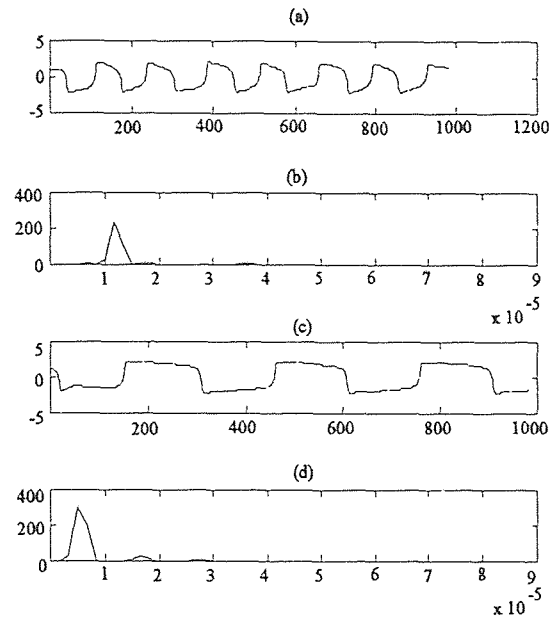


Figure 4.6 a) Velocity coupling (time series). b) spectral function. c) direct coupling (time series). d) spectral function. In both coupling modes $F_{xy} = F_{yx} = 0.2$, and $\mu_x = \mu_y = 2$.

These differences evolve from the nature of their interaction which affects the behavior of the two oscillators and their influence on each other. Selection of the characteristic frequencies for the two coupled oscillators was such to represent the bimodality of the circadian rhythms. The two frequencies always consisted of the fundamental and the second harmonic. For example, if the fundamental period was chosen to be 24 hours, the second period would be 12 hours.

The fundamental frequencies for:

$$T = 12 \text{ hours}$$

$$\frac{1 \text{ cycle}}{12 \text{ hrs}} \cdot \frac{0.08331 \text{ cycle}}{1 \text{ hr}} \cdot \frac{1 \text{ hr}}{60 \text{ min}} \cdot \frac{1 \text{ min}}{60 \text{ sec}} = 2.315 \cdot 10^{-5} \frac{\text{cycle}}{\text{sec}}$$

and for T = 24 hours

$$\frac{1 \text{ cycle}}{24 \text{ hrs}} \cdot \frac{0.04167 \text{ cycle}}{1 \text{ hr}} \cdot \frac{1 \text{ hr}}{60 \text{ min}} \cdot \frac{1 \text{ min}}{60 \text{ sec}} = 1.1574 \cdot 10^{-5} \frac{\text{cycle}}{\text{sec}}$$

4.4 Velocity Coupling Simulation

Many experiments suggest that the circadian rhythms are generated by two or more interacting oscillators.^[6] As indicated by our single Van der Pol oscillator simulation, we were unable to approach the real time activity data. The inability of the single dimensional Van der Pol oscillator to simulate circadian rhythms is related to the following facts:

- The frequency spectrum of the circadian activity data consisted of 2nd, 3rd, and higher harmonics which are not integer multiples of the fundamental frequency. Another oscillator is needed to account for these harmonics.
- The waveform structure of the circadian activity rhythms are nonlinear and complex in nature. In order for us to obtain similar waveforms from our model, our model should not be limited and should include other nonlinear parameters.

Prior to coupling the two oscillators, we determined the correction factors (ϵ_x and ϵ_y) needed to maintain the fundamental periods of the oscillators as the non-linear coefficients (μ_x and μ_y) were increased. Table 4.2 lists the corresponding values:

μ_x	μ_y	ϵ_x	ϵ_y
0	0	None	None
1.5	0.6	1.36	1.4
3	1	2	1.8
4	2	3	2.8
6	3	4	4

Table 4.2: The correcting factors (ϵ_x, ϵ_y) needed for different (μ_x, μ_y) values.

Our first attempt involved the coupling of two Van der Pol oscillators (velocity coupling). Figure 4.7 shows the structural diagram and equations for this particular mathematical model.

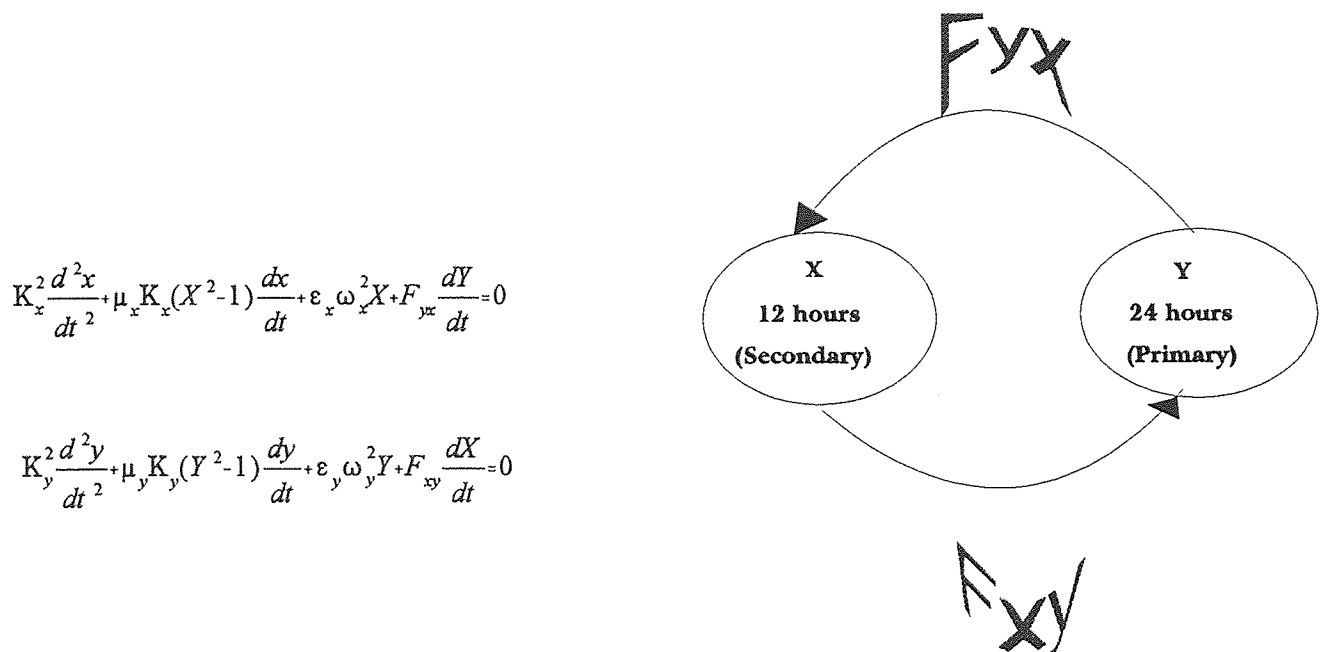


Figure 4.7 Structural diagram and equations for a mathematical model of hamsters' circadian activity system, consisting of two coupled Van der Pol oscillator model. F_{yx} coupling of Y onto oscillator X, F_{xy} coupling of X onto oscillator Y. μ_y, μ_x are the nonlinear coefficients of the Y and X oscillators respectively.

Since the fundamental period of the real activity data was approximately 24 hours, we let the period T for the Y oscillator be 24 hours. Since $\omega = \frac{2\pi}{T}$, $\omega_y^2 = 0.06854 \text{ rad/sec}^2$. We multiplied ω_y^2 by the correcting factor ϵ_y (for $\mu_y = 0.6$, $\epsilon_y = 1.4$) to account for the change in the Y oscillator's fundamental period as a result of μ_y . The remaining parameters were set to the following:

$\mu_x = 1.5$, $F_{xy} = F_{yx} = 0.2$, and $\omega_x^2 = 0.3728 \text{ rad/sec}^2$ with a correcting factor ($\epsilon_x = 1.36$, table 4.2). Figure 4.8 compares the results of the simulation and the real circadian activity data.

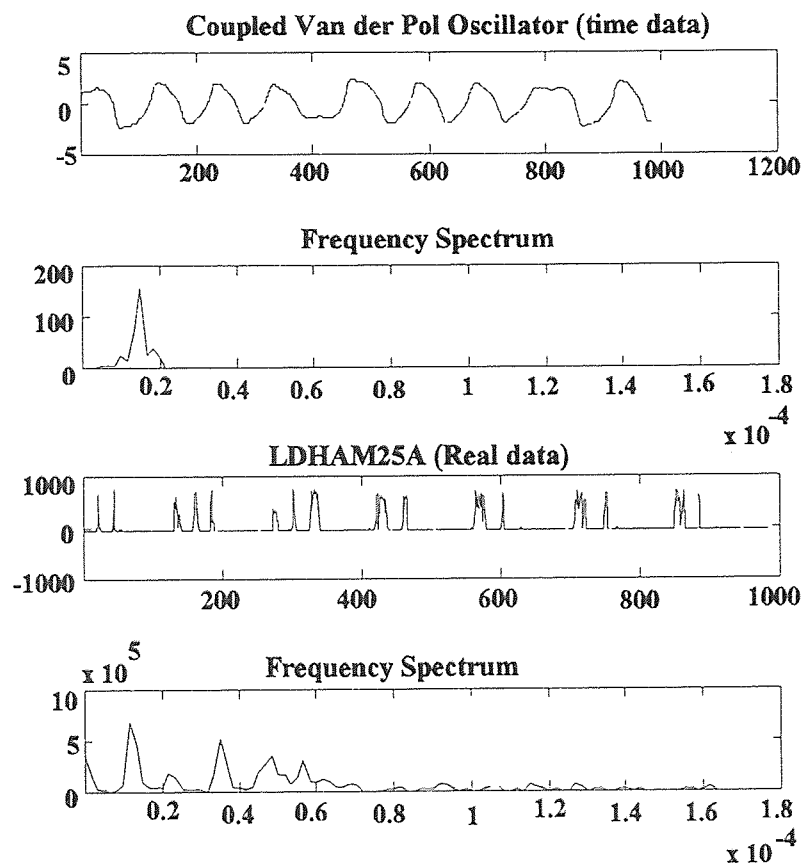


Figure 4.8 A comparison between the simulation and the real circadian activity data in time and frequency domains.

The comparison reveals the following differences:

1. The period (T) of the simulation is smaller than the period of the real activity rhythms.
2. The time series waveforms are dissimilar in shape and amplitude.
3. The spectral function of the real activity data is comprised of many harmonics unlike the spectral function of the simulation.

This particular mathematical model of velocity coupling is based on the work of Kronauer. In Kronauer's model, the two oscillators x and y drive two different activity rhythms - temperature and sleep wake.^[1] In our model we are assuming that both oscillators are contributing to only one rhythm (activity rhythm).

We tried to approach the real activity data in our model by continuously adjusting the non-linear coefficients and the strength of the coupling functions (F_{xy} , F_{yx}). Figure 4.9 shows the same model's output with 3 additional adjustments. First, the linear coupling drive (F_{xy}) of oscillator x onto oscillator Y was increased from 0.2 to 0.5. Second, the non-linear coefficient of oscillator Y (μ_y) was increased to 2.0. Third, the non-linear coefficient of oscillator X (μ_x) was increased to 3.0. The fundamental period of the real activity data was 24.26 hours,

$$\frac{1}{1.145 \times 10^{-5} \times 3600 \frac{\text{seconds}}{\text{hour}}} = 24.26 \frac{\text{hours}}{\text{cycle}}$$

while the fundamental period of the simulation data was 21.2 hours. The obvious advantage of this model is the introduction of the 2nd and higher harmonics as can be seen in figure 4.9. We continued adjusting the parameters to optimize the model but where

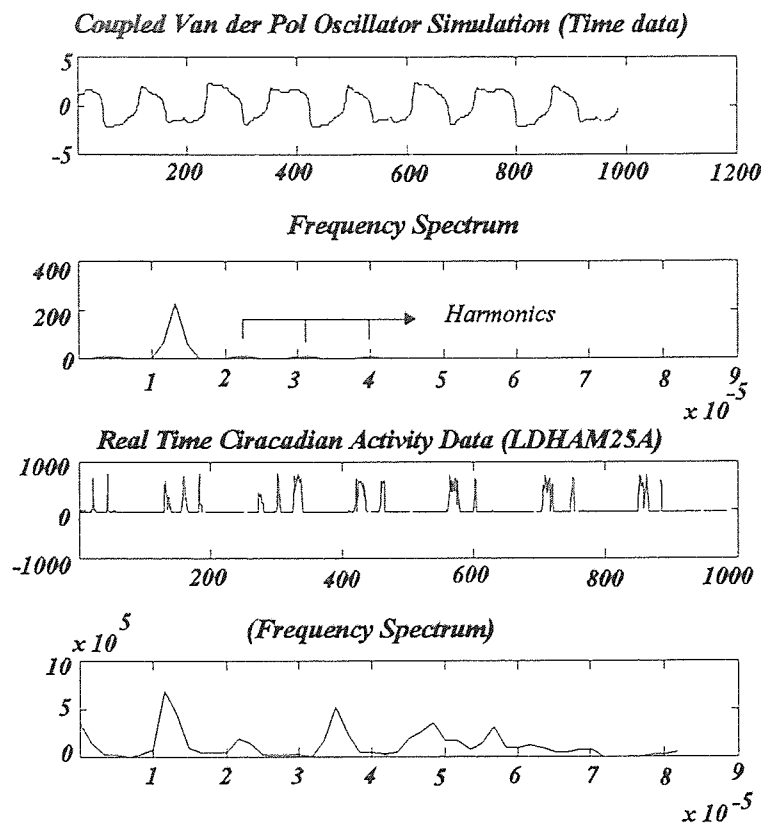


Figure 4.9 A comparison between the simulation and the real circadian activity rhythm. The model's parameters were set to the following values: $F_{xy} = 0.5$, $F_{yx} = 0.2$, $\mu_x = 3.0$, and $\mu_y = 2.0$.

unsuccessful in obtaining the desired outcome. Based on our results, we concluded that in the velocity coupling model, the increase of the coupling drive of the X oscillator onto the Y oscillator (F_{xy}) generated the required level of 2nd and higher harmonics.

Although the model improved, we were still unable to replicate the time series activity rhythms and the distinct appearance of their harmonics. In section 4.5, we will discuss an important factor which was introduced to the model and resulted in a substantial improvement of our model's output.

4.5 Ultradian Rhythms

In order to improve our coupled Van der Pol oscillator model, the discontinuity or intermittency observed in the hamsters' activity data cycles (time series) must be understood, and possibly associated to a physical behavior. Researchers believe that other higher frequency rhythms exist ($T \approx 2-16$ hours) that influence, or, are part of the circadian system, which drive such effects. These rhythms are referred to as *Ultradian Rhythms*.^[4] Ultradian rhythms have periods shorter than 16 hours. They can be produced by alterations in endogenous and exogenous factors. Ultradian rhythms have been observed in various rodents, and oscillations with periods of 2-4 hours have been discovered in hamsters and rats. Other theories exist and attempt to provide an understanding to these mechanisms. One such theory assumes an existence of an independent relaxation oscillator that produces these rhythms (the relaxation oscillator is a result of a substance in the body which fluctuates in concentration and is responsible for these consistent oscillations). The mechanisms still remain unknown.

Our ultradian rhythms model was associated with the relaxation oscillator model and we simulated ultradian rhythms as high frequency ($T=4$ hours) sawtooth-like waves. In order to accomplish this, a sawtooth function was first generated using MatLab which produced an ASCII file. Figure 4.10 shows the output waveform.

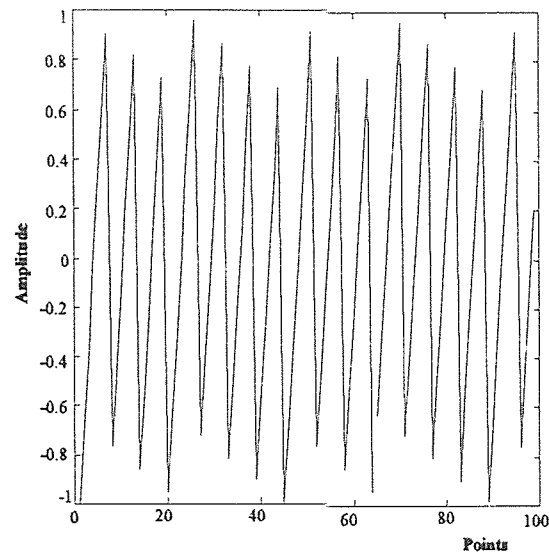


Figure 4.10 A 100 point Sawtooth waveform.

Second, the sawtooth data file was exported as an ASCII file to VisSim where it was modified . Modification of the sawtooth waveform consisted of the following:

- Noise was applied as a random gaussian function with 0 mean and a standard deviation of 1 to the model to simulate the substance's fluctuation (non-linear) in reaching its peak. This is especially important in order to establish a meaningful model that is linked to a physical process.
- The output is turned on (substance concentration is high) and off (substance concentration is low) at an equivalent time interval.

Figure 4.11 shows the results.

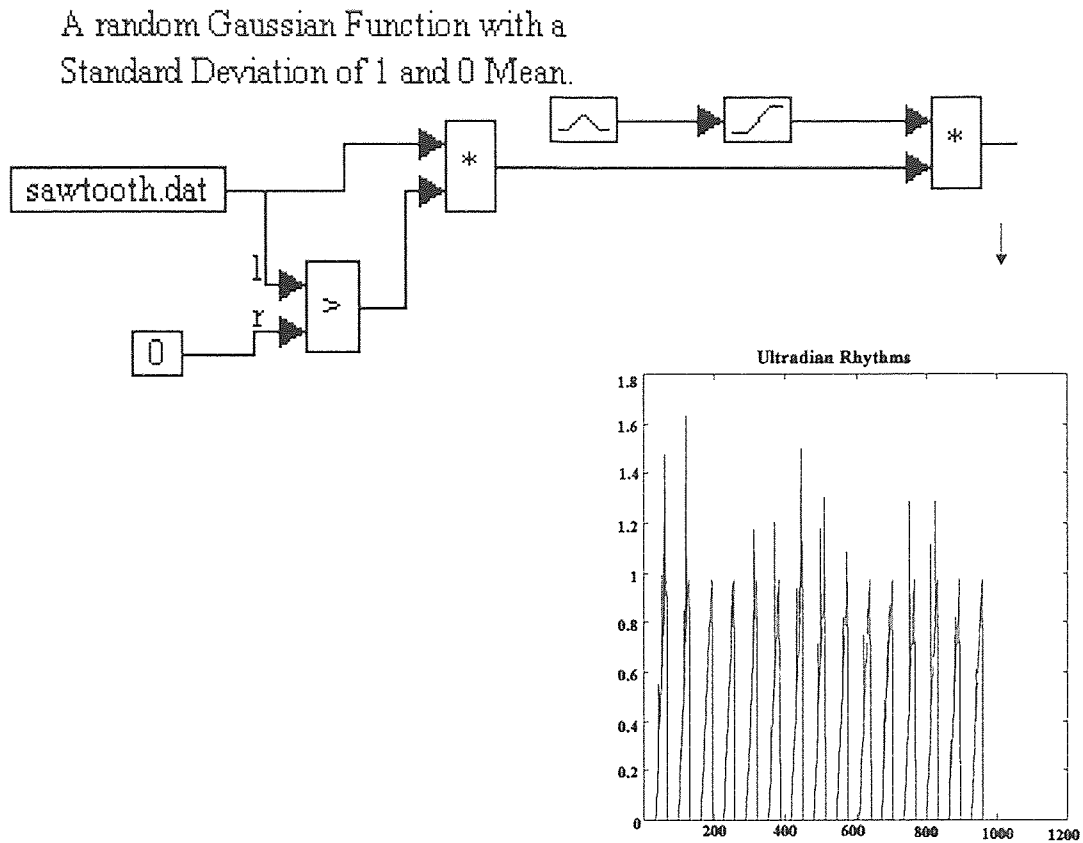


Figure 4.11 Ultradian Rhythms simulation. The fundamental period is 4 hours.

The relaxation oscillator was incorporated in our coupled Van der Pol oscillator model. Figure 4.12 shows the result of this modification and compares it to the real circadian activity data, and figure 4.13 shows the frequency spectrum comparison.

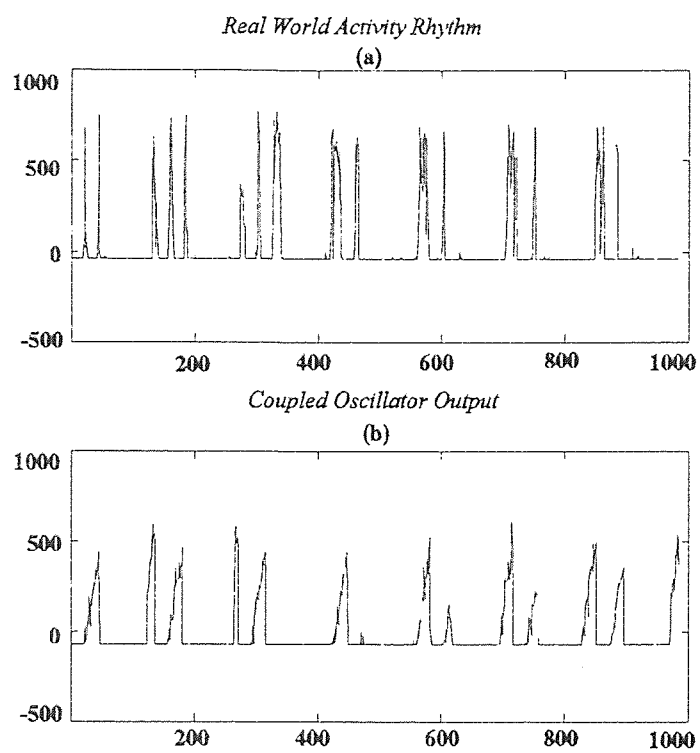
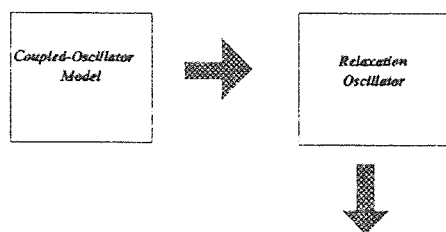


Figure 4.12 a) hamster's activity data (Light/Dark) cycle. b) Simulation results after the addition of the ultradian oscillator.

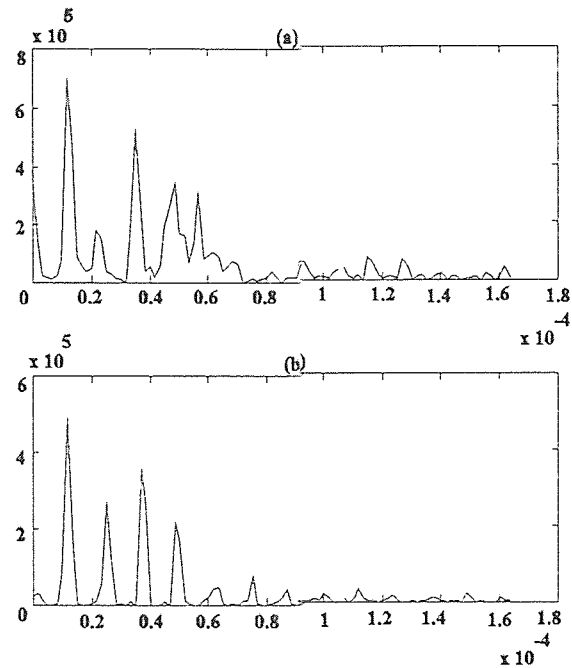


Figure 4.13 a) Frequency spectrum of hamster's activity data (Light/Dark) cycle. b) Frequency spectrum of coupled Van der Pol oscillator model.

The improvement of the model in simulating the circadian activity rhythms of hamsters, inspired us to use it for further analysis and to explore complex behaviors such as phase shifting and entrainment (discussed in chapter 5). Also, it justified the use of the coupled Van der Pol oscillator model and the capability of the model in simulating the circadian system in animals.

CHAPTER 5

ENTRAINMENT

5.1 Introduction

Daily entrainment which insures internal coupling and synchronization is an important and an active process. The phase and amplitude of circadian rhythms are related to both elapsed time and to certain repetitive events that occur daily. Temporal isolation or non-entrainment and entrainment studies suggested distinct phase relationships among circadian rhythms. In 1965, Aschoff reported that free-running humans showed significantly different periods in their circadian rest-activity and core temperature rhythms. This phenomenon has been termed spontaneous internal desynchronization.^[13] Other non-entrainment studies demonstrated a phase advance of REM (Rapid Eye Movement) sleep, performance and alertness fell and reached a minimum prior to the self-selected sleep onset time. Biological organisms developed daily activity-sleep cycles with periods slightly greater or less than the circadian cycle (24 hours) and biological oscillators became desynchronized (have different periods). The preferred free-running period was approximately 25 hours, and prolonged sleep episodes up to 18 hours occurred in normal human subjects. On the other hand, when biological organisms were entrained by the 24 time cues (*Zeitgebers*), they developed a 24 hour activity- rest cycle, human subjects had a normal pattern of cortisol secretion, and performance remained high prior to sleep onset

time. Biological oscillators became synchronized as well.

An environment with or without time schedules such as lights out, lights on and meal times and other scheduled behaviors can confine or release the biological oscillators. In the case of our experimental hamsters another constraint or schedule was added which was the limited access to the tread mill apparatus.

Many studies suggest that entrainment of the circadian system can be accomplished by applying external stimuli to the endogenous biological oscillators. By selecting the proper period and amplitude of the external stimulus, it can control the phase and rhythm of the biological oscillators "During entrainment, the self -exciting oscillator adopts the period of the driving periodic stimulus and maintains a particular phase relation with the entraining cycle."^[1] Environmental synchronizing cycles have been identified in various experiments. These environmental cycles include ambient temperature, electromagnetic field strength, food availability, social cues, and light-dark (LD) cycles. In our two-coupled oscillator model we incorporated an artificial zeitgeber agent (sinusoidal function) which simulated the real environmental LD cycle. Basically, this was accomplished by adding an external input (cosine function) that turned on and off for the duration of the specified intervals. For example, in order to simulate a 12h. light/ 12h. dark cycle, the cosine function was attached to the two-coupled oscillator model (using a switch) and generated an output at the specified frequency and amplitude for 12 hours. It was then, disengaged (0 output) for the rest of the cycle's duration (12 hours).

In our work, we will examine the effects of the simulated zeitgeber on our model's performance and attempt to provide a detailed comparison between the model's output and each of the LD experimental circadian activity data.

5.2 Understanding Entrainment

Figure 5.1 shows the activity data obtained from various hamsters. Each hamster was subjected to a unique condition. Hamster #17B (figure 5.1a) was kept in continuous dark cycle for 28 days. Hamster #26a (figure 5.1b) was subjected to a light stimulus for

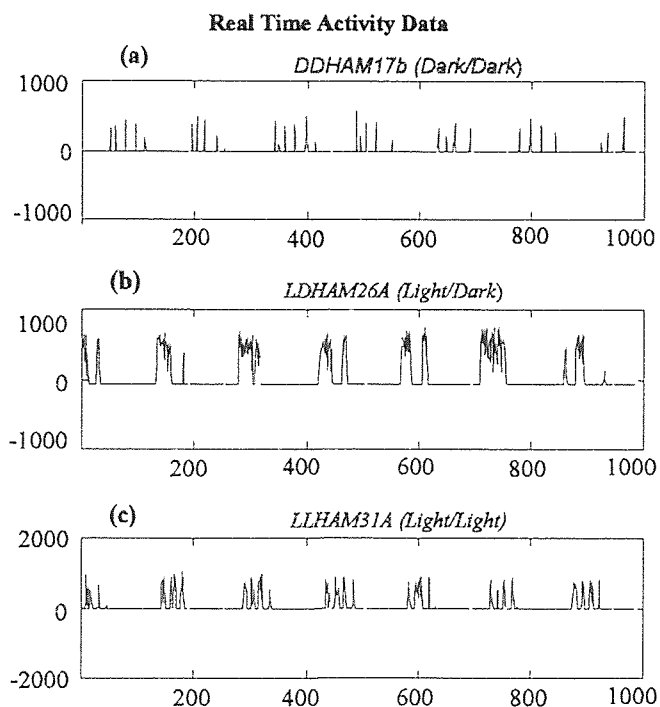


Figure 5.1 Activity data of various hamsters placed in different environments. a) Dark/Dark. b) Light/Dark. c) Light/Light

14 consecutive days and then the stimulus was removed and the hamster was kept in dark for an additional 14 days. Hamster #31a (figure 5.1c) was kept under a light stimulus for 28 days. Figure 5.2 shows the correspondent frequency spectrums. In the case of the dark/dark condition, the fundamental frequency was 23.76 hours while the other conditions had slightly different fundamental frequency which was 24.76 hours.

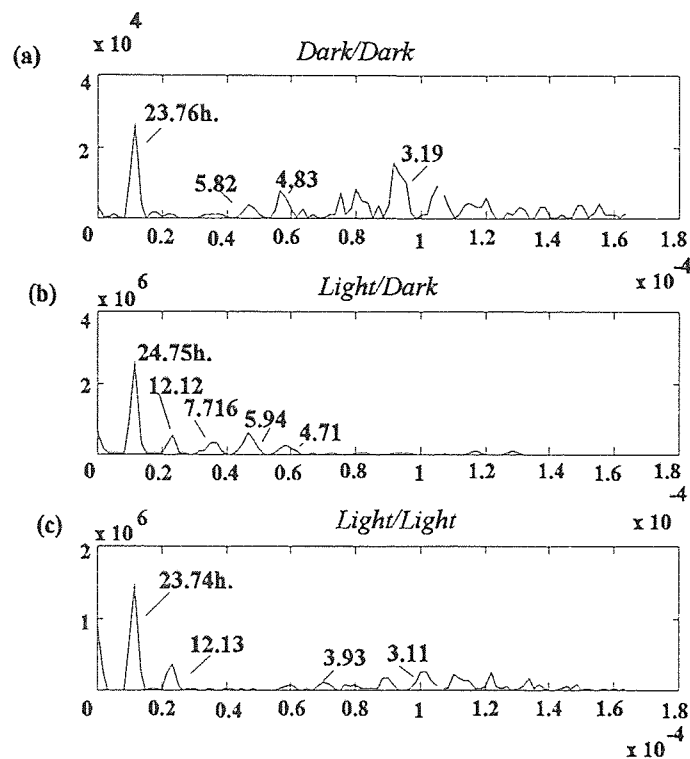


Figure 5.2 Spectral functions.

In order for us to simulate entrainment, an external input was applied to our coupled oscillator model. This input was connected and was removed at different hours.

In one of the simulations, a cosine wave with a period of 24 hours was applied to our Van der Pol coupled-oscillator model for a simulated duration of 240 hours and then was removed for another 240 hours. Such behavior simulated the transition from light to dark. Mathematically, this is equivalent to the following:

$$K_y^2 \frac{d^2 y}{dt^2} + \mu_y K_y (Y^2 - 1) \frac{dy}{dt} + \epsilon_y \omega_y^2 Y + F_{xy} \frac{dX}{dt} = E(t) \quad (5.1)$$

$$K_x^2 \frac{d^2 x}{dt^2} + \mu_x K_x (X^2 - 1) \frac{dx}{dt} + \epsilon_x \omega_x^2 X + F_{yx} \frac{dY}{dt} = 0 \quad (5.2)$$

$E(t) = A \cos \omega(t)$ where A is the amplitude of the stimulus, μ , the nonlinear parameter of the system, and K , the fixed time parameter. $E(t)$ (external stimulus) is not confined to a cosine function, it can be any other periodic stimulus.

We will first derive some assumptions which will be extracted from our single Van der Pol oscillator analysis example. We begin by applying an external input which acts on the nonlinear Van der Pol equation. This system is described by the following equation:

$$K_x^2 \frac{d^2 x}{dt^2} + \mu_x K_x (X^2 - 1) \frac{dx}{dt} + \omega_x^2 X + F_{yx} \frac{dY}{dt} = E(t) \quad (5.3)$$

Where $E(t) = A \cos \omega(t)$. If we assume that μ (the nonlinearity parameter) is very small ($\mu \approx 0$), the system can be approximated by the following solution:

$$K_x \frac{d^2 x}{dt^2} + \omega_x^2 X = E(t) \quad (5.4)$$

$$X(t) = A \sin \omega t + B \cos \omega t + G \cos \varpi t \quad (5.5)$$

where $G = \frac{A}{\omega^2 - \varpi^2}$, A and B are constants, ω is the natural frequency of the system (intrinsic), G and ϖ are the amplitude and frequency of the external input (extrinsic) respectively. As can be seen, the solution will be dominated by the $\cos \varpi t$ term if either A is large or the two frequencies difference ($\Delta = \omega^2 - \varpi^2$) is small. Theoretically, in order for entrainment to occur, the following three assumptions are fundamental to our model:

- $\Delta \omega$ (the frequency difference) is relatively small.
- $E(t)$, the external input, is not confined to a cosine function. The stimulus' wave shape is irrelevant.
- The external input is directly acting on the primary oscillator Y and indirectly (by means of coupling) on the secondary oscillator X .

We assumed that $\omega = 0.2856$ rad (22 hours), the natural frequency) of the endogenous oscillator, and $\varpi = 0.2618$ (24 hours) rad, the frequency of the external stimulus. First, we simulated the single Van der Pol oscillator model without the external input. Next, we performed the same simulation with the external input applied and acting on the model.

Figures 5.3 and 5.4 show the results of VisSim simulation in the time domain. Figure 5.5 shows the spectral function analysis.

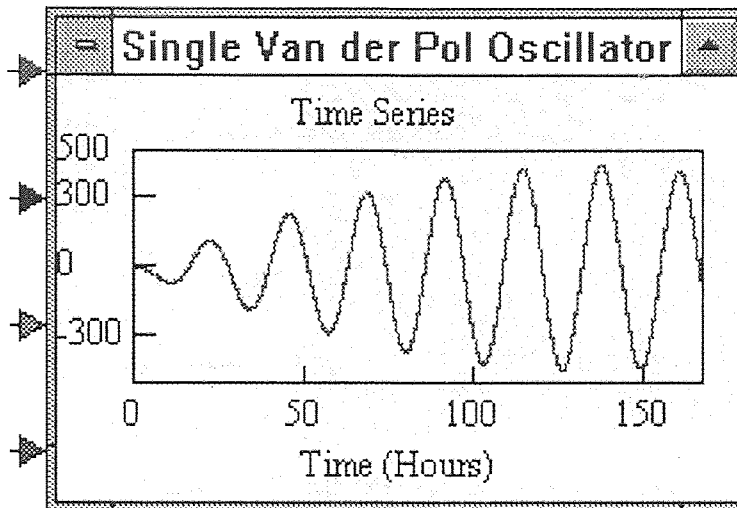


Figure 5.4 Time series simulation of the single Van der Pol oscillator with an external stimulus acting on it.

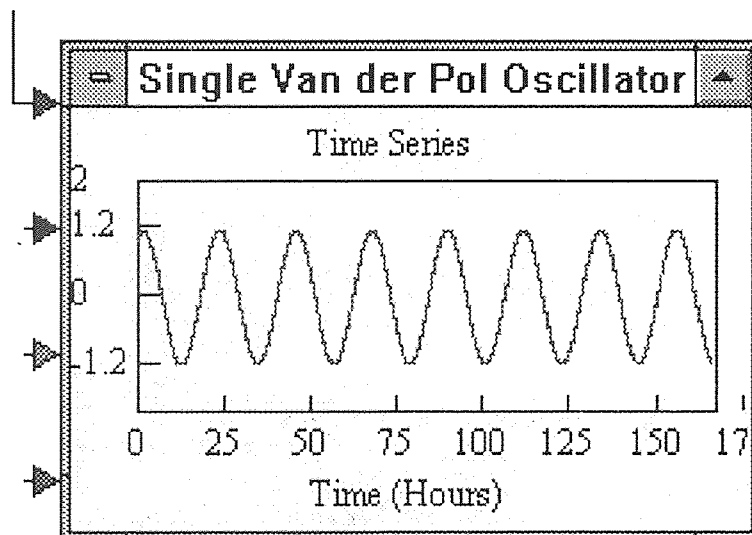


Figure 5.3 Time series simulation of the single Van der Pol oscillator model with no external stimulus.

For this particular case, where $\mu = 0$, $A = 3$, $T_i = 22$ hours (period of the endogenous oscillator), and $T_e = 24$ hours (period of the external stimulus), the resulting oscillation's frequency was very close to the frequency of the external stimulus.

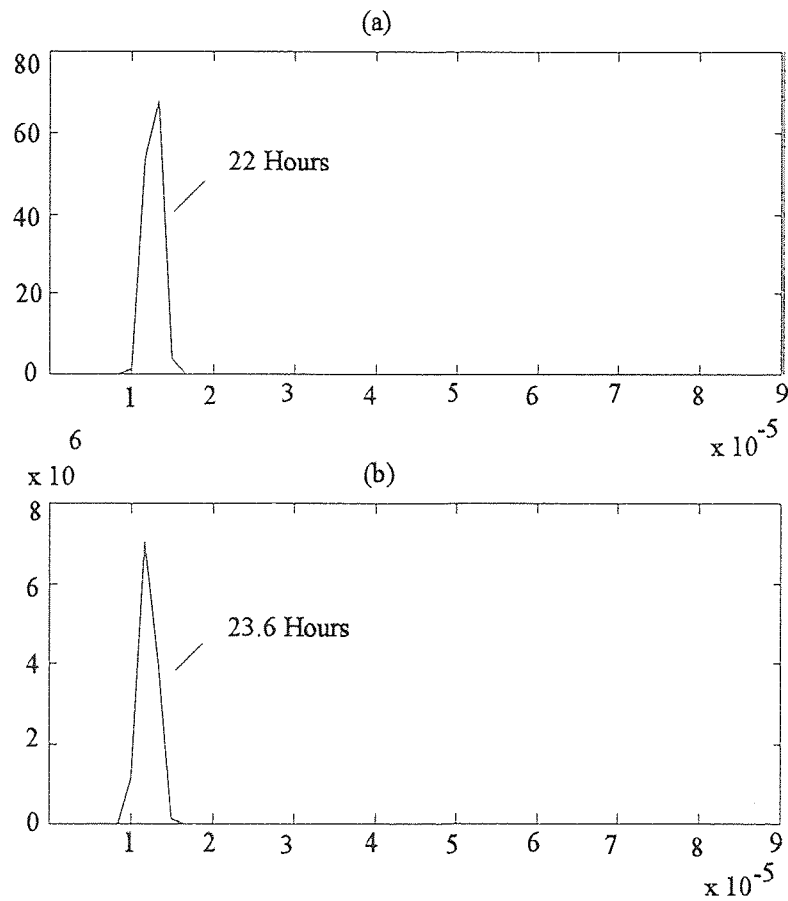


Figure 5.5 Spectral functions. a) Single Van der Pol oscillator, $\omega = 0.2856$ rad (22 hours) the natural frequency of the model. b) Single Van der Pol oscillator with an external stimulus applied to it. $\varpi = 0.2618$ rad (24 hours) the frequency of the external stimulus.

Previous researchers work revealed several factors that influenced the quality of

entrainment.^[1] Mainly, entrainment is affected by three fundamental elements:

- Frequency of the external stimulus.
- Amplitude of the external stimulus (directly proportional to entrainment).
- Nonlinearity of the system (μ). The larger the nonlinearity, the easier the system can be entrained.

5.3 Light/Dark to Dark/Dark Transition

In order to obtain real entrained data to be able to compare it with our model's results, various experimental hamsters were subjected to distinct entrainment environments. For example, 3 experimental hamsters were exposed to a light/dark environment (lights on for 12 hours and lights out for 12 hours) for a period of 14 days. After the 14 days, lights were removed and the hamsters were kept in continuous dark for an additional 14 days.

Since activity data was acquired at a sampling rate of $\frac{144 \text{ Samples}}{24 \text{ hr}}$, $14 \text{ Days} * \frac{144 \text{ Samples}}{\text{Day}} = 2016 \text{ Samples}$, we expect the transition to occur roughly around that point. Figure 5.6 shows the time series data. As can be seen from the figure, there is a change in the waveform shape and amplitude around the 2016 Sample. In order to further explore the data, the FFT was applied to the time series data and the frequency spectrum was plotted before and after the transition. Figure 5.7 shows the time series sections (before and after transition) and figure 5.8 shows the fundamental and sub-harmonics frequencies for the two sections.

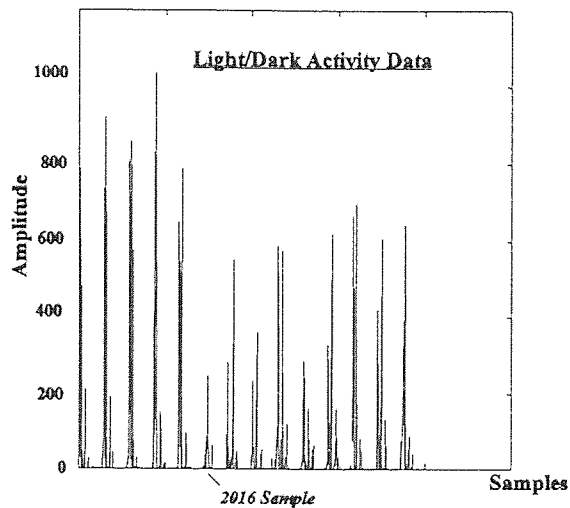


Figure 5.6 Time series activity data of an experimental hamster. The point labeled 2016 Sample is the point of transition from Light/Dark to Dark/Dark.

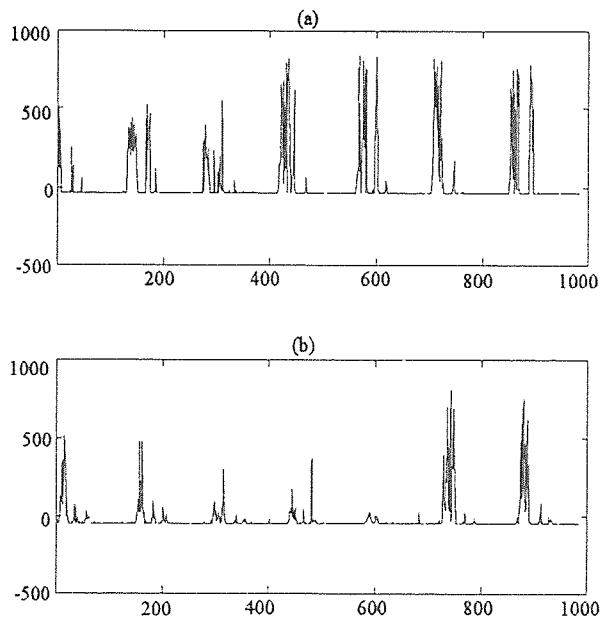


Figure 5.7 Time series plot of the activity data (light/dark to dark/dark transition). a) Light/dark
b) Dark/dark.

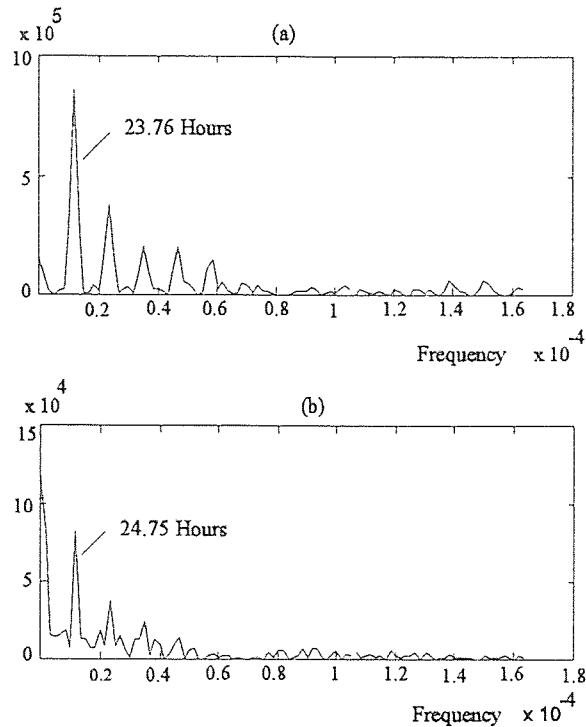


Figure 5.8 Spectra light/dark to dark/dark transition. a) Spectra of the light/dark section which shows a fundamental period of 23.76 hours. b) Spectra of the dark/dark section which shows a fundamental period of 24.75 hours.

A simple explanation for the fundamental period change in the two sections is that the hamster adopted the period of the driving external stimulus (light/dark environment) and maintained a phase relationship with this particular entraining cycle. As we release him from this entraining cycle, the hamster preferred to run at his free-running period of his endogenous oscillator which was (24.76 hours).

Shi Ziong Yang^[1] performed considerable work on entrainment and arrived at several important conclusions. His results revealed that, in order for entrainment to

occur, there is a lower stimulus amplitude threshold level and this level varies with different values of μs (nonlinearity parameters) and $\Delta \omega$ (the difference between the endogenous oscillators natural frequency and the external input's frequency). For example, when the amplitude of the external stimulus was less than 0.1, entrainment did not occur. Also, as we have seen in chapter 3, as we increased μ , the natural frequency of the system was shifted. This shift in the natural frequency will certainly introduce further complications to the model.

5.4 Entrainment Simulation

We begin by introducing our Van der Pol coupled oscillator model incorporating the external stimulus. Figure 5.9 shows VisSim representation of the model, and figure 5.10 shows a block diagram of the entire model.

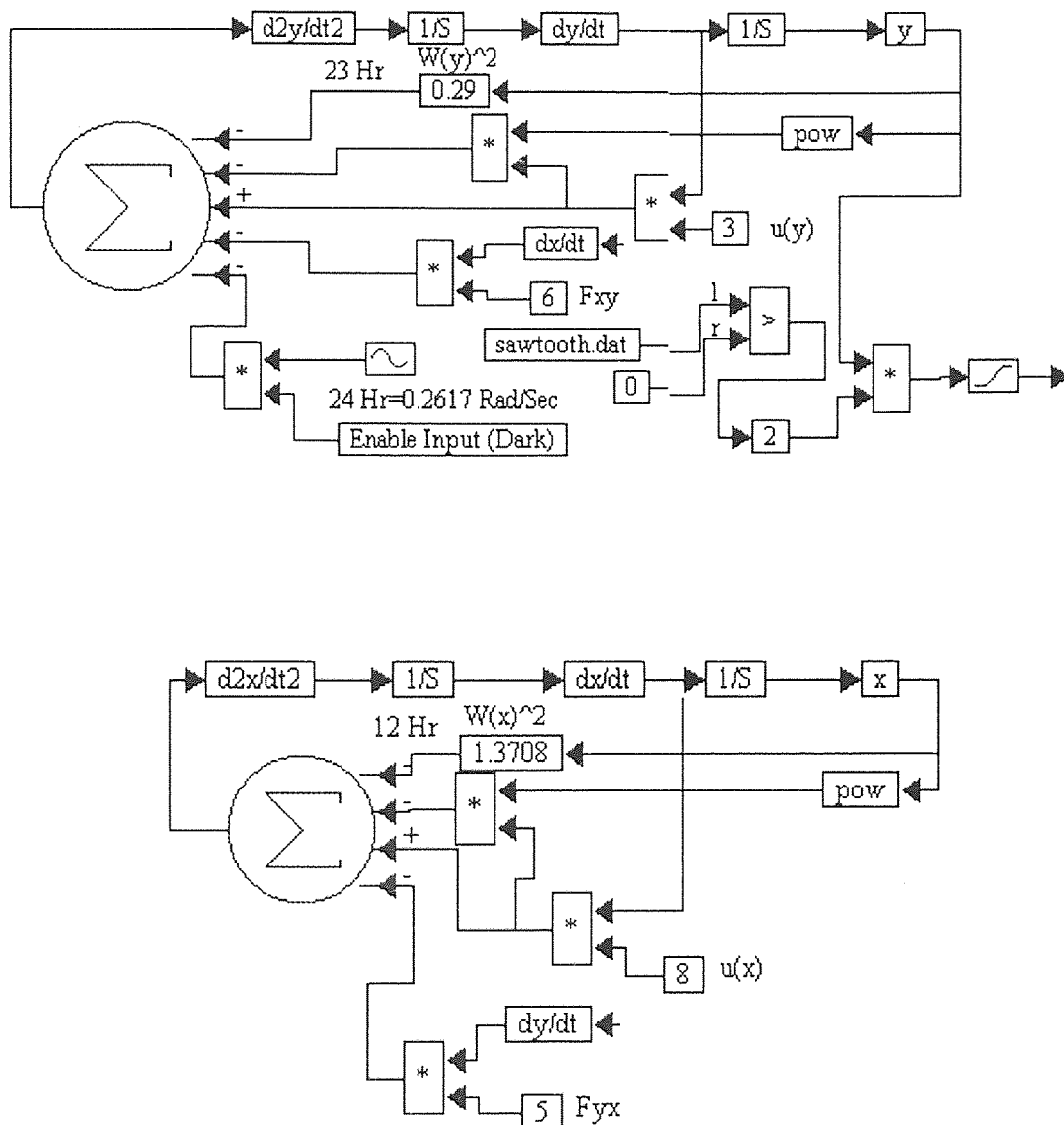


Figure 5.9 VisSim presentation of the Van der Pol coupled-oscillator model. The model include an external input which was applied and removed at specified intervals.

$$K_y^2 \frac{d^2 y}{dt^2} + \mu_y K_y (Y^2 - 1) \frac{dy}{dt} + \epsilon_y \omega_y^2 Y + F_{xy} \frac{dX}{dt} = E(t)$$

$$K_x^2 \frac{d^2 x}{dt^2} + \mu_x K_x (X^2 - 1) \frac{dx}{dt} + \epsilon_x \omega_x^2 X + F_{yx} \frac{dY}{dt} = 0$$

$$Z(t) = Y(t) + R(t)$$

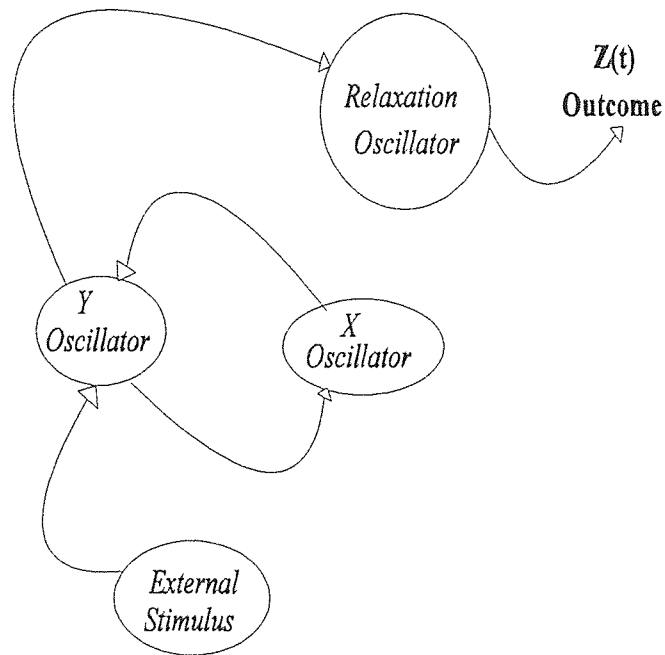


Figure 5.10 Structural diagram and equations for the final mathematical model.

The free-running period of the coupled oscillator model was determined to be 22.2 hours prior to applying the external stimulus. We assigned the external stimulus a period of 24 hours. In order to simulate entrainment, we engaged the external stimulus for a simulated period of 240 hours and then removed it for an additional 240 hours. We then used the spectral function as a tool to determine the entrainment characteristics. As figure 5.11-a shows, the coupled internal oscillators were entrained by the

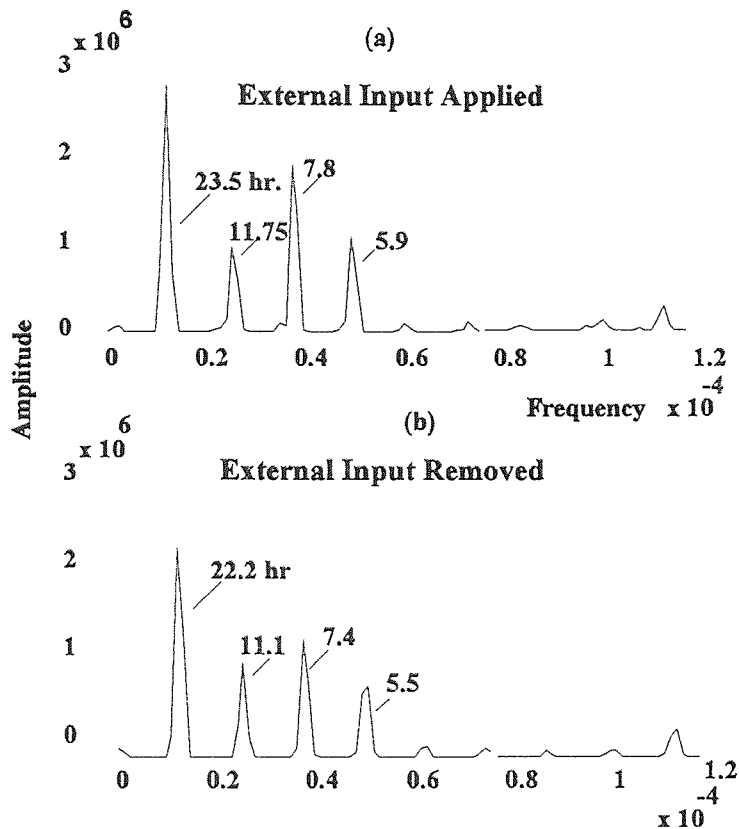


Figure 5.11 Coupled oscillator model a) External input with a period of 24 hours was applied for 10 simulated days. The figure shows the fundamental frequency and the harmonics. b) After 10 simulated days the input was removed and the system was allowed to free-run.

external input. Synchronization took place as the period of the system approached the period of the external input(24hr). As the external input was removed and the coupled internal oscillators were free-running, desynchronization took place (between the external stimulus and the coupled internal oscillators), and the period of the system was restored to its original period (22.2hr). It should be noted that synchronization will occur only if the period of the external oscillator is close to the free-running oscillator or an integer multiple or submultiple of it. Synchronization did not occur when the period of the two oscillators were very different from each other. Figure 5.12 is the real circadian activity data and figure 5.13 is the model's output.

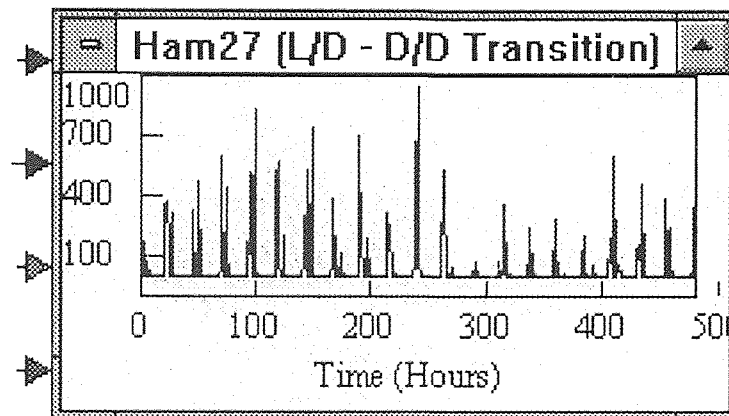


Figure 5.12 Records of real circadian activity data.

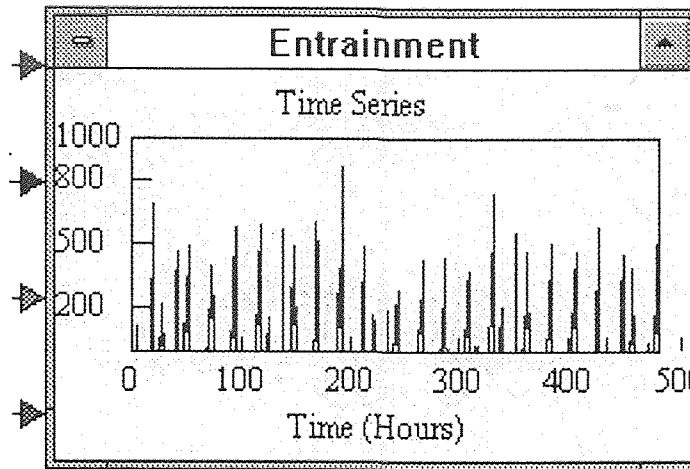


Figure 5.13 Simulation output.

5.5 Light/Light to Dark/Dark Transition

In this experiment, a hamster was subjected to a light stimulus continuously for 14 days. Then, the light stimulus was removed and the hamster was kept in a dark environment for 14 days. Figures 5.14 and 5.15 show the frequency spectrums before, after, and during the transitional phase. As a consequence of the transition, the circadian activity period was shifted by approximately 1 hour 24.75hr. Light/Light vs 23.8hr. Dark/Dark), additional harmonics were introduced or became more prominent, and the amplitude of the spectrum became smaller.

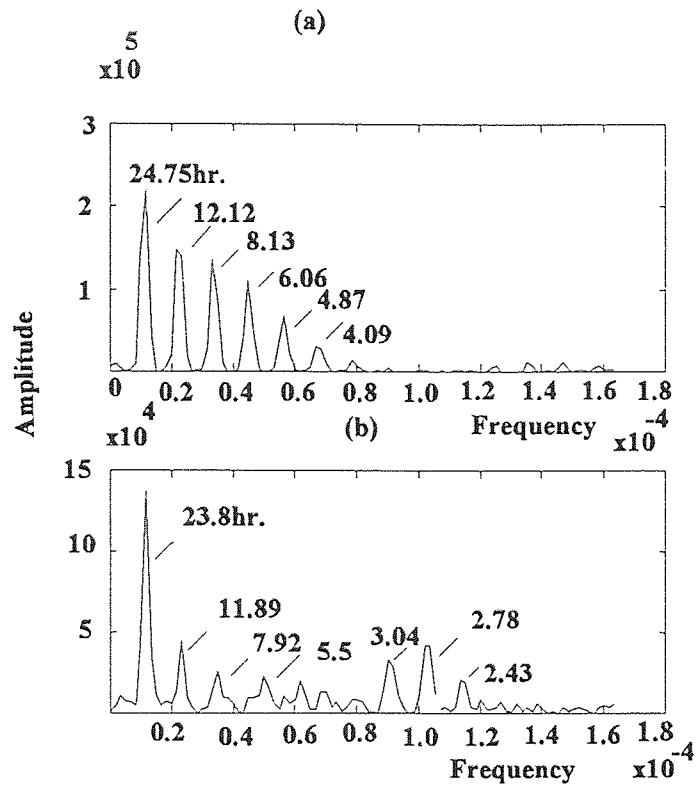


Figure 5.14 Frequency Spectrum of time series activity data.
a) Light/Light before transition. b) Dark/Dark after transition.

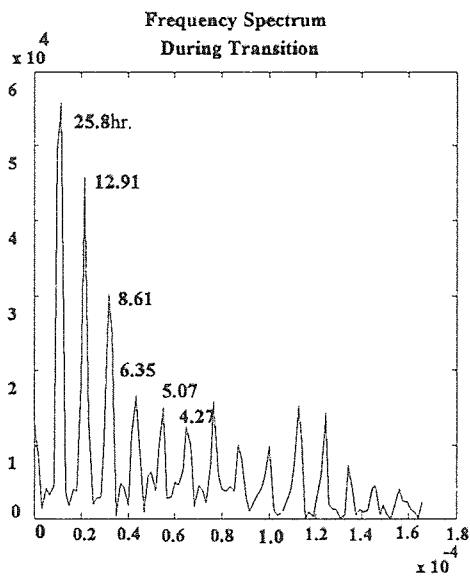


Figure 5.15 Frequency spectrum of time series activity data during the transitional phase from Light/Light to Dark/Dark.

CHAPTER 6

CONCLUSIONS

6.1 Summary

In an effort to understand complex systems and processes such as the circadian system, different means have to be employed. Our main tool for understanding such a system was accomplished by mathematically modeling the circadian activity process of various hamsters. The mathematical model was established and developed based on the knowledge of previous researchers work in this field, and on our acquired real circadian activity data. A data collection system was developed in order to obtain the hamster's circadian activity data. The data was pre-processed and analyzed in both time and frequency domains in order to initiate bases for the basic mathematical model. For example, our data frequency spectral analysis showed that the circadian rhythms frequency structure consisted of harmonics and sub-harmonics. We used the frequency characteristics of the circadian rhythms as our building block in developing our model. Our main objective and emphasis was to develop a flexible mathematical model that will approach the real circadian activity rhythms. After successfully accomplishing this task, the model was further enhanced to simulate more complex phenomena such as entrainment.

Existing circadian rhythm models did not utilize ultradian rhythm pacemakers. As our model showed, ultradian rhythms were essential to the model's structure in order to approach the real circadian activity data in both the time and frequency domains. Through frequency spectral analysis, we acquired valuable knowledge about the activity circadian rhythms' characteristics. For instance, we showed that the main frequency peak of the activity rhythms always occurred at approximately 24 hours which was accompanied by 2nd 3rd and higher harmonics. We investigated the effect of the nonlinearity on the system's harmonic structure. As we increased the nonlinearity coefficient (μ), the harmonic amplitude increased. Also, the frequency spectrum showed the bimodality (two distinct frequency components) that exists in the circadian rhythms.

We investigated entrainment which is fundamental to the circadian system. This was accomplished by obtaining complex circadian activity data. The data contained information about the transition from synchrony to desynchrony by subjecting the hamsters to an external stimulus at specific time intervals. We were able to simulate these transitions by applying an external stimulus to our model. As the nonlinearity of our system increased, the system was easier to entrain. In fact, we were able to fully entrain the system by correctly setting its frequency and parameters.

In summary, based on our results we can state that the circadian system is regulated by complex endogenous interacting oscillators. These oscillators are normally synchronized by specific environmental cycles as discussed in previous chapters, and our coupled-oscillator model has the capacity of simulating the hamster's activity circadian

system and perhaps other circadian systems in temporal isolation and in artificial zeitgeber cycles. The success of our simulation can open unlimited paths for future development.

6.2 What May Come?

We can never emphasize enough the importance of circadian pacemakers and rhythms especially in human beings. The circadian system has a large influence in controlling our health, and mental activities. It is of great interest medically and economically to solve many disorders (shift work, jet lag, sleep disorders etc.,) that influence us and minimize our productivity and have an adverse effect on our health. We have not yet reached the end of the road; actually we have just started our journey in exploring circadian rhythms. The circadian oscillators are nonlinear and complex in nature. With the continuous advancement in technology and computer techniques, it is easier than ever to obtain complicated solutions for complex equations. More mathematical models have to be considered and studied, and these models should not be restricted to two interacting oscillators. Also, several other techniques such as coherence and bispectrum have to be employed in order to fully understand the system. Bispectrum will assist in further analyzing the phase relationship between harmonics of circadian rhythms, and coherence to obtain any correlation that exists between different rhythms.

Appendix A

Temperature Filter

```
#include <stdio.h>
#include <ctype.h>
#include <stdlib.h>
#include <string.h>

#define MAXLIN 20
#define FILTER SIZE 5
#define MAX NAME SIZE 20
#define CR 0x0D
#define LF 0x0A

main(argc,argv)

int argc;
char *argv[];

{
    FILE *fptr, *file out;
    char string[MAXLIN];
    char out string[MAXLIN];
    char name[MAX NAME SIZE];
    int count=0, value=0, loop=0;
    int number[FILTER SIZE];
    int temp number[FILTER SIZE];
    int top, search, temp;
    int numb,i;

    if(argc != 2)
        {
            (printf("Format: c>filter filename"));
            exit(1);
        }
    if( (fptr=fopen(argv[1], "r")) == NULL)
        {
            printf("Cannot open file %s.", argv[1]);
```

```

    exit(1);
}
strcpy(name,argv[1]);
for (i=0 ; i < MAX NAME SIZE ; i++)
{
    if (name[i] == '.')
    {
        name[i]=0x00;
        break;
    }
}
strcat(name, ".flt");
file out = fopen(name, "w");

while( loop==0 )
{
    if (count > 0)
    {
        for ( numb = 0; numb < FILTER SIZE-1; numb++)
        {
            number[numb] = number[numb+1];
            temp number[numb] = number[numb];
        }
        if (fgets(string, MAXLIN, fptr) == NULL)
            exit(1);
        number[FILTER SIZE-1] = atoi(string);
        temp number[FILTER SIZE-1] = number[FILTER SIZE-1];
        count++;
    }
    if (count == 0)
    {
        for ( numb = 0; numb < FILTER SIZE; numb++)
        {
            fgets(string, MAXLIN, fptr);
            number[numb] = atoi(string);
            temp number[numb] = number [numb];
            count++;
        }
    }
    for ( top = 0 ; top < FILTER SIZE - 1 ; top++)
        for ( search = top + 1; search < FILTER SIZE ; search++)
            if (temp number[search] < temp number[top])
                {

```

```
        temp = temp number[top];
        temp number[top] = temp number[search];
        temp number[search] = temp;
    }
if( (temp number[FILTER SIZE/2] < 450) && (temp number[FILTER SIZE/2]
> 380) )
    {
    temp number[FILTER SIZE/2] = temp number[FILTER SIZE/2] - 426;
    itoa(temp number[FILTER SIZE/2], out string, 10);
    fputs(out string, file out);
    fputc(CR, file out);
    fputc(LF, file out);
    printf("mid value of array[%d] is %d.\n",count,temp number[FILTER SIZE/2]);
    }
}
fclose(fpnr);
fclose(file out);}
```

MatLab Example File

```
#####
# This program is used to compare VisSim simulation Vs the hamster's activity data (12h.
# light/12h. dark).
#####

coupled=coupled-mean(coupled);
n=2000;
W=hanning(n);
subplot(4,1,1),plot(coupled,'b');
C=W.*(coupled(1:2000));
C1=fft(C(1:2000));
f=0.00167*(0:(length(C1)-1)/2)/length(C1);
P=C1.*conj(C1)/length(C1);
subplot(4,1,2),plot(f(1:50),P(1:50),'b');
load c:\hamsters\ldham25a.asc;
ldham25a=ldham25a-mean(ldham25a);
subplot(4,1,3),plot(ldham25a(1:2000),'b');
C2=W.*(ldham25a(1:2000));
C3=fft(C2(1:2000));
P1=C3.*conj(C3)/length(C3);
subplot(4,1,4),plot(f(1:50),P1(1:50),'b');
```

Simulation of a Single Van der Pol Oscillator Using VisSim

To help the reader understand our Van der Pol oscillator simulation, one point must be kept in mind: VisSim does not provide a differential function block. Instead, VisSim provides an integration function block. All the differential equations had to be transferred into ones that use integration operators. Therefore, to enter an ordinary differential equation (ODE) in VisSim, first algebraically solve the equation for the highest derivative, and insert the number of integrator blocks that equals the order of the highest derivative. For example, to simulate a single Van der Pol oscillator (equation A.1), the following steps have to be accomplished.

$$K^2 \frac{d^2x}{dt^2} + \mu K(x^2 - 1) \frac{dx}{dt} + \omega^2 x = 0 \quad (\text{A.1})$$

- Algebraically solve the equation for the highest derivative
- In VisSim, insert the number of integrator blocks that equals the order of the highest derivative.

Assuming that $K = 1$ (the fixed time parameter) and algebraically solving the equation for the highest derivative, the equation is equivalent to:

$$\frac{d^2x}{dt^2} = -\mu x^2 \frac{dx}{dt} + \mu \frac{dx}{dt} - \omega^2 x \quad (\text{A.2})$$

Since the highest derivative is of second order, we need to insert two integrator blocks in VisSim.

- Convert the original equation into a form that can be entered into VisSim. For the single Van der Pol equation we need the following VisSim blocks:
 1. Two integrator blocks (second order differential equation)
 2. Two multiplication blocks
 3. Three variable blocks ($\frac{d^2x}{dt^2}, \frac{dx}{dt}, x$)
 4. A power block (x^2)
 5. A constant block (μ)
 6. A gain block (ω)
 7. A summation block
 8. A plot block

After wiring the blocks and inserting the blocks in their proper positions, the simulation shown in figure A.1 results.

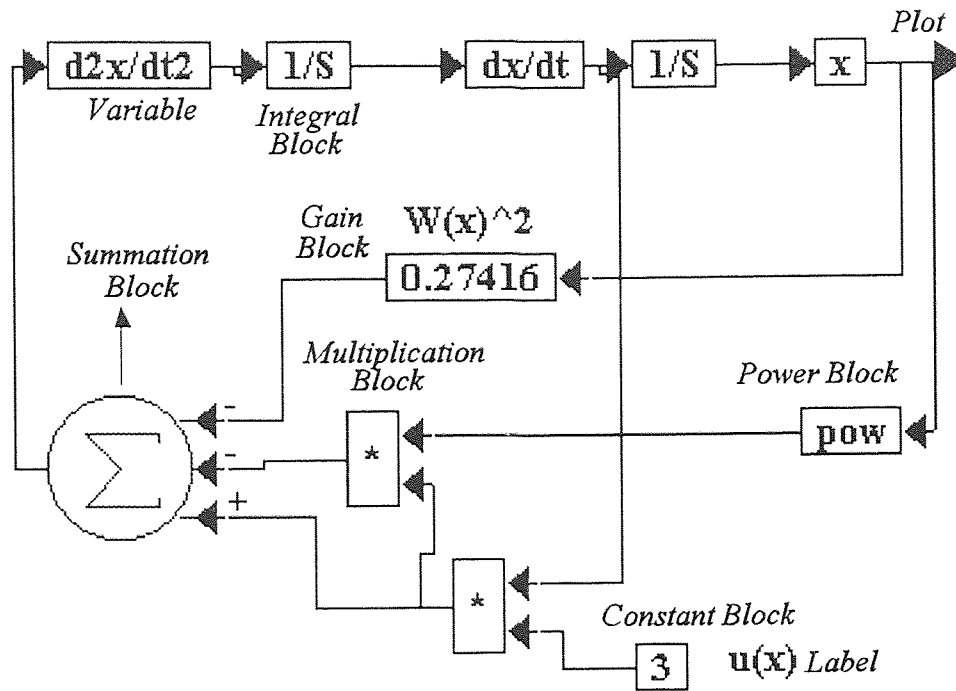


Figure A.1 VisSim model of the single Van der Pol oscillator.

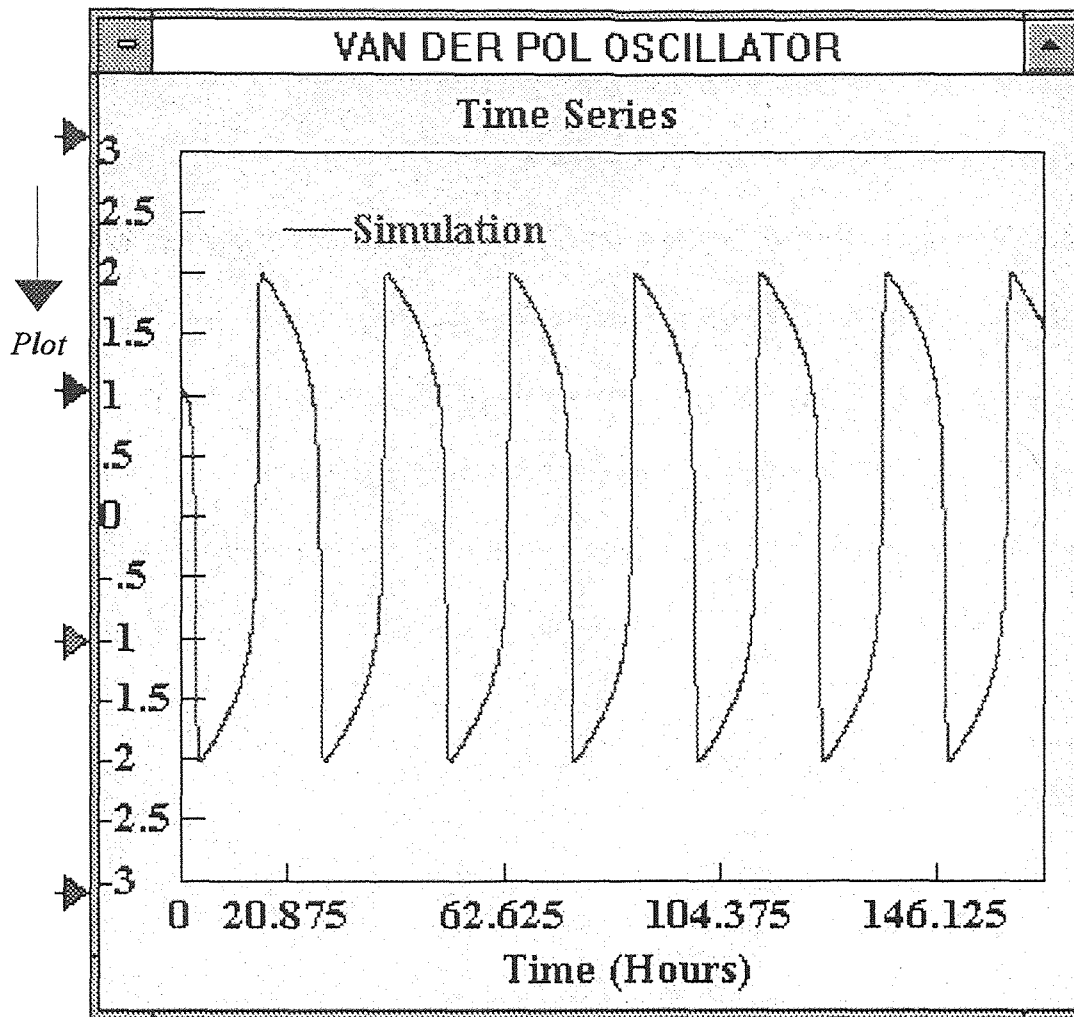


Figure A.2 Output of the single Van der Pol oscillator simulation, $\mu = 3.0$, and $T = 24$ hours.

Figure A.2 is the output waveform of the simulation. If needed, rearrange the blocks for better viewing. To satisfy the original equation (equation A.1), set the value of the constant, power, and gain blocks to the desired values.

Prior to simulation, set the simulation parameters. From the Simulate Menu, choose

Change Parameters and set the Range Start, End and Step Size. In our model, the step size ($\Delta\tau$) was set to 0.0167. This value originates from the real time sampling rate, $\frac{6\text{Samples}}{\text{Hour}} \cdot \frac{1\text{Hour}}{60\text{Minutes}} \cdot \frac{1\text{Minute}}{60\text{Seconds}} = 0.00167$ Sample/Second. If the step size value was chosen to be 0.00167, it will produce too many points. In order to limit the number of our simulated data points, a step size of 0.0167 was selected. The simulated data points can be collected via an *export block*. VisSim provides such a block in order to export ASCII data. The fixed interval for exporting data can be adjusted. For example, in our simulation, $\Delta\tau = 0.0167$ sample/sec., range start = 0, and range end = 480. This will force the simulation to generate 28742 data points. If we set the fixed interval parameter in the export block to 0.167, only 2874 data points will be written to the file.

REFERENCES

- [1] Yang, Shi Ziong, "*Circadian Rhythms*," Ph.D. dissertation, New Jersey Institute of Technology, May 1990.
- [2] Weitzman, Elliot D, *Chronobiology of Man*. New York: Springer-Verlang, 1983.
- [3] Czeisler, Charles A., Weitzman, Elliot D., Moore-Ede, Martin C., Zimmerman, Janet C., and Knauer, Richard S., "Human Sleep: Its Duration and Organization Depend on Its Circadian Phase," *Science*, vol. 210, pp. 12, 1980.
- [4] Refinetti, R. and Menaker, M., "The Circadian Rhythm of Body Temperature," *Physiology & Behavior*, vol. 51, pp. 613-637, 1992.
- [5] Daan, S. and Berde, C., "Two Coupled Oscillators: Simulations of the Circadian Pacemaker in Mammalian Activity Rhythms," *Journal of Theoretical Biology*, vol. 208 pp. 297-313, 1978.
- [6] Winfree, Arther T., "Biological Rhythms and the Behavior of Populations of Coupled Oscillator," *Journal of Theoretical Biology*, pp. 15-42, 1967.
- [7] Strughold, Hubertus, *Your Body Clock*. New York: Charles Scribner's Sons, 1971.
- [8] Weston, Lee, *Body Rhythm*. New York and London: Harcourt Brace Jovanovich, Inc., pp. 4, 119-130, 1972.
- [9] Orlock, Carol, *Inner Time*. New Jersey: A Birch Lane Press Book, 1993.
- [10] Gittelson, Bernard. *Biorhythm*. New York: Arco Publishing Company, pp. 2-22, 1977.
- [11] Hughes, Martin, *Body Clock*. New York: Facts On File Inc., 1992.
- [12] Turek, Fred W. "Circadian Principles and Design Rotating Shift Work Schedules," *The American Physiological Society*, vol. 251, pp. 636-637, 1986.

- [13] Gander, Philippa H, Kronauer, Richard E., Czeisler, Charles A., and Moore-Ede, Martin C. "Simulating the Action of Zeitgebers on a Coupled Two-Oscillator Model of the Human Circadian System," *The American Physiological Society*, vol. 247, pp. 418-425, 1984.
- [14] Gander, Philippa H., Knauer, Richard E., Czeisler, Charles A., and Moore-Ede, Martin C. "Phase Shifting Two Coupled Circadian Pacemakers: Implications for Jet Lag," *The American Physiological Society*, vol. 249, pp. 705-719, 1985.
- [15] Jilge, Burghart, Hornicke, Heiko, and Stahle, Herbert. "Circadian Rhythms of Rabbits During Restrictive Feeding," *The American Physiological Society*, vol. 253, pp. 46-53, 1987.
- [16] Winget, Charles M., DeRoshia, Charles W., Markley, Carol L., and Holley, Daniel C. "A Review of Human Physiological and Performance Changes Associated with Desynchronization of Biological Rhythms," *Aviation, Space, and Environmental Medicine*, vol. 55 pp. 1085-1096, December 1984.
- [17] Flokard, Simon, Wever, Ruther A., and Wildgruber, Christina M., "Multi-oscillatory Control of Circadian Rhythms in Human Performance," *Nature*, vol. 305, pp. 223-226, September 1983.
- [18] Zimmerman, Janet C., Philippa H., Knauer, Richard E., Czeisler, Charles A., Moore-Ede, Martin C., and Weitzman, Elliot D. "Human Sleep: Its Duration and Organization Depend on Its Circadian Phase," *Science*, vol. 210, pp. 1264-1267, December 1980.
- [19] Ronda, Joseph M., Knauer, Richard E., Czeisler, Charles A., and Moore-Ede, Martin C., "*Thirteen Chronobiological Disorders: Analytic and Therapeutic Techniques*," pp. 297-329.
- [20] Brady, John, "Circadian Rhythms - Endogenous or Exogenous?" *Journal of Comparative Physiology A*, vol. 161, pp. 711-714, 1987.
- [21] Hayashi, Chihiro, *Nonlinear Oscillations in Physical Systems*. New Jersey: Princeton Press, 1985.
- [22] McCarley, Robert W., "A Limit Cycle Mathematical Model of the REM Sleep Oscillator System," *American Physiological Society*, vol. 251, pp. 1012-1021, 1986.

- [23] Gander, Philippa H, Kronauer, Richard E., Czeisler, Charles A., and Moore-Ede, Martin C., "Modeling the Action of Zeitgebers on the Human Circadian System: Comparisons of Simulations and Data," *The American Physiological Society*, vol. 247, pp. 427-443, 1984.